DOI: https://10.83080/rejost.vol6no4.295

Researchers Journal of Science and Technology (REJOST)

Integrated Seismic Attribute–Driven Reservoir Characterization and Hydrocarbon Prospect Evaluation in the "X" Field, Niger Delta Basin

Samuel T. Ebong*; Aniekan M. Ekanem; Nyakno J. George and Ndifreke I. Udosen

Abstract

This study presents an integrated seismic attribute and petrophysical approach for reservoir characterization and hydrocarbon prospect evaluation in the X-Field, Niger Delta Basin, Nigeria. The research was undertaken to reduce the uncertainties associated with structural complexity, fault-controlled compartmentalization, and hydrocarbon distribution within the field. While several studies in the Niger Delta have focused independently on structural interpretation or petrophysical analysis, limited attention has been given to the combined application of multi-seismic attributes and quantitative volumetric ranking for improved prospect delineation and uncertainty reduction. The X-Field is located within the extensional tectonic province of the Niger Delta and is characterized by listric growth faults, synthetic and antithetic fault systems, and rollover anticlines that form multiple fault-assisted closures. Interpretation of 3D post-stack seismic data integrated with well logs, well tops, and check shot data led to the identification and correlation of two major reservoir units, RES N and RES O, within the Agbada Formation. Structural interpretation delineated nine prospective closures (A–I) with closure areas ranging from 77.62 to 231.71 acres and gross rock volumes between 4,968.75 and 18,575.58 acre-ft. Petrophysical analysis revealed average net-to-gross ratios of 0.78–0.79, effective porosity values between 0.23 and 0.25, and water saturation ranging from 0.15 to 0.17, indicating generally good reservoir quality across the field. RES N exhibited slightly better reservoir characteristics compared to RES O. Seismic attribute analyses involving RMS amplitude, variance, sweetness, AVO fluid strength, and relative acoustic impedance identified high-amplitude and low-impedance anomalies concentrated around structurally elevated zones and rollover anticlines, suggesting hydrocarbon-charged reservoir sands and effective trap integrity. Deterministic volumetric estimation using formation volume factors of Bo = 1.25 and Bg = 0.8 produced Stock Tank Oil Initially in Place (STOIIP) values ranging from 351, 050.05 to 1, 178, 700.55 BOE and Gas Initially in Place (GIIP) values between 5,171, 361.37 and 19,622,939.84 MSCF. Total Hydrocarbons Initially in Place (HIIP) ranged from 5, 522, 411.42 to 20,801,640.38 BOE, with Prospect A showing the highest hydrocarbon potential, followed by Prospects E and D. The integrated results demonstrate that hydrocarbon accumulation within the field is predominantly controlled by growth fault-related rollover anticlines and fault-bounded structural closures. The study highlights the effectiveness of combining multi-seismic attributes, petrophysical evaluation, and volumetric analysis for improved reservoir characterization and prospect ranking in structurally complex deltaic environments.

✉ Samuel T. Ebong: sirphysicsonline@gmail.com; samuelebong@aksu.edu.ng

[1]Department of Physics, Akwa Ibom State University, Ikot Akpaden, Mkpat Enin, Akwa Ibom State, Nigeria

Keywords: Reservoir, Seismic, Attributes, Hydrocarbon, Volumetric

Article history
Received: March 23, 2026
Received in revised form: May 24, 2026
Accepted for publication: May 30, 2026
Available online: June 1, 2026

1.0 Introduction

The Niger Delta Basin, located along the Gulf of Guinea in West Africa, is one of the world's most prolific hydrocarbon provinces and a major contributor to Nigeria's petroleum resources. The basin covers more than 300,000 km² and extends from the Benin flank in the west to the Calabar hinge line in the east (Ekanem & Ebong 2026; Doust & Omatsola, 1990). It developed as a passive continental margin following the Late Jurassic-Cretaceous separation of the African and South American plates, which was followed by thermal subsidence and the accumulation of thick sedimentary sequences during the Paleogene and Neogene periods (Ebong et al., 2023). The stratigraphy of the Niger Delta consists of three major lithostratigraphic units: the Akata, Agbada, and Benin Formations (Uwa et al., 2019, George et al., 2022a, b; Udosen et al., 2024a; Ekanem et al., 2024). The Akata Formation is composed mainly of marine pro-delta shales and serves as the primary source rock (Evamy et al., 1978). Overlying this unit is the Agbada Formation, which contains interbedded sandstones and shales deposited in deltaic and shallow marine environments and forms the main hydrocarbon reservoirs of the basin. The uppermost Benin Formation consists largely of continental sands deposited under alluvial conditions (Short & Stauble, 1967, Attai et al., 2015, George & Bassey, 2018; Umoh et al., 2025). Structurally, the basin is dominated by syn-sedimentary deformation caused by gravitational instability resulting from rapid sediment loading over the ductile Akata shales (Attai et al.., 2025). This process generated listric growth faults, rollover anticlines, and fault-dependent closures that form the primary hydrocarbon traps in the region (Doust & Omatsola, 1990). The complex structural framework and rapid lateral facies variations typical of deltaic environments often complicate reservoir delineation and hydrocarbon prospect evaluation.

Seismic reflection data remain essential for subsurface characterization; however, conventional interpretation may not adequately resolve subtle stratigraphic features and reservoir heterogeneities. Seismic attribute analysis provides an effective means of enhancing seismic interpretation by extracting quantitative information related to amplitude, phase, frequency, and reflector continuity (Brown, 2011, Chopra & Marfurt, 2007). When integrated with well data, seismic attributes can reveal structural features, delineate reservoir boundaries, and highlight amplitude anomalies associated with potential hydrocarbon accumulations (Barnes, 2016).

The "X" Field, located within the Niger Delta Basin, exhibits structural and stratigraphic characteristics typical of deltaic hydrocarbon systems. Accurate evaluation of its hydrocarbon potential requires detailed characterization of reservoir distribution and trapping mechanisms. This study applies seismic attribute analysis integrated with structural interpretation and well log data to evaluate the hydrocarbon prospectivity of the field. The objectives are to delineate the structural framework, analyze key seismic attributes, and identify potential hydrocarbon-bearing zones within the study area. Despite extensive hydrocarbon exploration within the Niger Delta Basin, uncertainties associated with fault-controlled reservoir compartmentalization, seismic amplitude ambiguity, and structural complexity continue to affect accurate prospect delineation and volumetric estimation. Previous studies in the basin have largely emphasized either conventional seismic structural interpretation or standalone petrophysical analysis, with limited

integration of multi-seismic attribute techniques for simultaneous reservoir characterization, hydrocarbon prediction, and quantitative prospect ranking. Furthermore, the combined application of variance, sweetness, RMS amplitude, relative acoustic impedance, and AVO fluid strength attributes for prospect evaluation within structurally complex rollover anticline systems remains insufficiently explored in the X-Field. Therefore, this study integrates seismic attributes, structural interpretation, petrophysical evaluation, and deterministic volumetric estimation to reduce exploration uncertainty and improve hydrocarbon prospect identification within the field.

The novelty of this study lies in the integration of multiple seismic attributes with structural interpretation, petrophysical characterization, and volumetric prospect ranking to improve hydrocarbon prediction within a structurally complex Niger Delta field. Unlike previous studies that focused primarily on individual seismic attributes or conventional structural mapping, this work combines variance, RMS amplitude, sweetness, AVO fluid strength, and relative acoustic impedance analyses to simultaneously delineate fault architecture, reservoir continuity, hydrocarbon indicators, and prospect ranking. The study further integrates these results with deterministic volumetric estimation to establish the relative hydrocarbon potential of identified fault-bounded closures.

2.0 Location and Geology of the Study Area

The "X" Field is located within the shallow offshore sector of the Niger Delta Basin, Nigeria, along the Gulf of Guinea. The Niger Delta lies between latitudes 3°N and 6°N and longitudes 2°E and 9°E (Figure 1), covering an area of approximately 70,000 km². It represents one of the largest deltaic systems in the world and hosts significant hydrocarbon accumulations within its thick sedimentary sequences (Doust & Omatsola, 1990; Tuttle et al., 1999).

The basin developed as a passive continental margin following the Late Jurassic–Early Cretaceous rifting associated with the separation of the African and South American plates (Atat et al., 2013). Subsequent thermal subsidence and sustained sediment supply from the Niger–Benue River system resulted in the progradation of a large deltaic complex during the Paleogene to Recent periods (George et al., 2025). Sediment thickness within the basin exceeds 10 km in some areas, reflecting high rates of clastic sedimentation (Evamy et al., 1978).

The stratigraphic framework of the Niger Delta comprises three major lithostratigraphic units: the Akata, Agbada, and Benin Formations (George et al. 2020, George, 2021; Udosen et al., 2024b, c). The basal Akata Formation consists predominantly of marine pro-delta shales with minor turbiditic sands and is interpreted as the principal source rock for hydrocarbons within the basin (Ekanem & Ebong 2025; Evamy et al., 1978). Overlying this unit is the Agbada Formation, composed of interbedded sandstones and shales deposited in delta-front, distributary channel, and shallow marine environments (George & Thomas, 2023). These sandstone bodies constitute the primary hydrocarbon reservoirs in the Niger Delta petroleum system (Short & Stauble, 1967; Doust & Omatsola, 1990). The uppermost Benin Formation consists mainly of continental sands deposited in fluvial and alluvial environments (George &Thomas, 2024).

Structurally, the Niger Delta is dominated by gravity-driven deformation caused by the differential loading of rapidly deposited deltaic sediments over the under compacted Akata shales (George et al., 2017). This process generates extensive listric growth faults, rollover anticlines, shale diapirs, and fault-dependent closures that act as major hydrocarbon trapping mechanisms (Doust & Omatsola, 1990, Obianwu et al., 2025). Reservoir units within the Agbada Formation are commonly compartmentalized by these growth fault systems, creating structurally controlled hydrocarbon accumulations. The "X" Field exhibits structural and stratigraphic characteristics typical of Niger Delta hydrocarbon fields, where

reservoir distribution and hydrocarbon entrapment are strongly influenced by fault-controlled structural closures and deltaic sedimentary architecture.

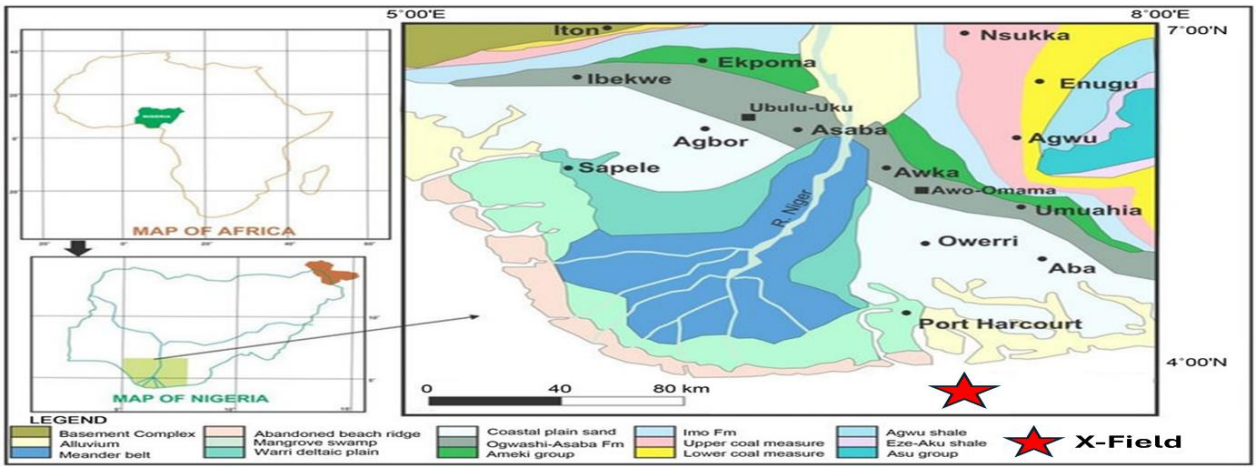

Figure 1: Map of the Niger Delta basin showing the location of X-field (After Nwanjide 2013)

3.0 Materials and Methods

The datasets used in this study include post-stacked 3-D seismic data, digitized logs in LAS format (including gamma ray, acoustic, density, neutron, and resistivity), check shots, and deviation statistics data. These datasets were analyzed and interpreted using Schlumberger Petrel, interactive petrophysics, and Microsoft Excel.

3.1 Methodology

The methodological workflow adopted in this study, as shown in Figure 2, integrates well log analysis, seismic interpretation, and seismic attribute analysis to evaluate hydrocarbon prospectivity in the "X" Field, Niger Delta Basin. The analysis was carried out using Petrel for seismic interpretation and attribute generation, while petrophysical analysis was performed using Interactive Petrophysics. The workflow consisted of data loading and conditioning, well log normalization, reservoir identification and petrophysical evaluation, seismic interpretation, seismic - to - well calibration, attribute analysis (including both surface and volume attributes), and volumetric estimation of hydrocarbons.

The study commenced with the loading and conditioning of available datasets. A new project was created in Petrel, and the coordinate reference system (CRS) corresponding to the Niger Delta region was defined to ensure spatial consistency of the datasets. The post-stack 3D seismic data in SEG-Y format were imported with the correct survey parameters, including inline and crossline ranges, sampling interval, and trace length. Quality control procedures were performed to confirm the integrity, polarity, and orientation of the seismic cube. Well data consisting of well headers, deviation surveys, check-shot data, and log curves (gamma ray, resistivity, density, neutron, and sonic logs) were then imported in LAS format. The well headers established the geographic positions of the wells within the seismic grid, while deviation surveys defined the well trajectories. Check-shot data provided time–depth relationships necessary for accurate seismic-to-well calibration.

Well log normalization was subsequently performed to ensure consistency of log responses across the wells. Variations in logging tools and acquisition conditions often result in inconsistencies in log measurements; therefore, normalization ensures that logs from different wells are comparable. In this study, gamma ray logs were normalized within a range of 1–150 API, resistivity logs between 0.2–2000 Ωm, density logs between 1.65–2.65 g/cc, neutron porosity between 0–0.60, and sonic logs between 40–140 µs/ft. The normalization process improved the reliability of lithological interpretation and reservoir correlation across the wells.

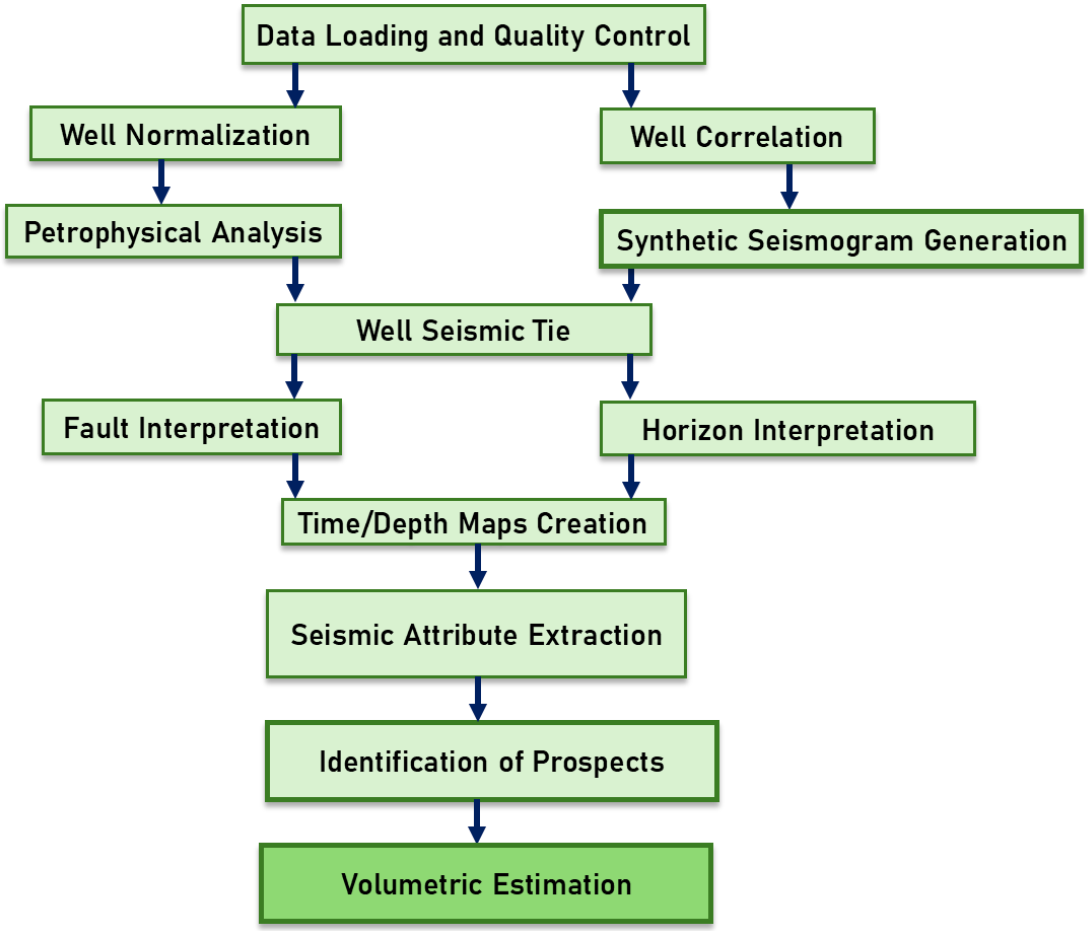

Figure 2: Workflow design for the study

Reservoir identification and correlation were carried out using the integrated responses of the gamma ray, resistivity, density, neutron, and sonic logs. The gamma ray log was primarily used to distinguish sand from shale intervals, with low gamma ray readings indicating clean sand bodies and high readings representing shale units. Resistivity logs were used to identify hydrocarbon-bearing intervals, which typically exhibit higher resistivity compared to water-saturated formations (Ekanem et al., 2021a; Ebong., et al 2023). The combined interpretation of density and neutron logs aided in determining lithology and porosity variations. Using these log signatures, reservoir tops and bases were identified and correlated across the wells (Horsfall et al., 2024). The correlation established the lateral continuity and thickness variations of the reservoir units within the field and led to the identification of two principal reservoirs designated as Reservoir N and Reservoir O.

Petrophysical evaluation of the reservoirs was conducted to quantify reservoir quality and hydrocarbon potential. Key parameters estimated include shale volume, porosity, water saturation, permeability, and net-to-gross ratio. Shale volume was estimated from the gamma ray log using the Larionov equation for Tertiary rocks. The gamma ray index was first computed using equation 1 as shown below:

$$I_{GR} = \frac{GR_{log} - GR_{min}}{GR_{max} - GR_{min}} \qquad (1)$$

where GR_{log}= gamma ray reading of the formation, GR_{min}= minimum gamma ray in clean sand, and GR_{max}= maximum gamma ray in shale. The shale volume was calculated from equation 2 as shown below:

$$V_{sh} = 0.083(2^{3.7I_{GR}} - 1) \qquad (2)$$

Net reservoir thickness was determined by applying cut-off parameters of gamma ray ≤ 75 API, porosity ≥ 0.10, and water saturation ≤

0.60. The net-to-gross ratio (NTG) was then calculated using equation 3.

$$NTG = \frac{h_{net}}{h_{gross}} \quad (3)$$

where h_{net}= total thickness of net sand and h_{gross}= total gross reservoir thickness. Porosity was estimated using equation 4 from density logs using the density-porosity relationship.

$$\phi = \frac{\rho_{ma} - \rho_b}{\rho_{ma} - \rho_f} \quad (4)$$

where ρ_{ma} is matrix density (2.65 g/cc for sandstone), ρ_b is bulk density, and ρ_f represents formation fluid density. Water saturation was estimated using the Archie equation (Archie, 1942) as shown in equation 5:

$$S_w^n = \frac{aR_w}{\phi^m R_t} \quad (5)$$

where S_w= water saturation, R_w= formation water resistivity, R_t= true formation resistivity, n= saturation exponent (usually 2), a and m are constants as previously defined. Hydrocarbon saturation was subsequently calculated from equation 6.

$$S_h = 1 - S_w \quad (6)$$

Permeability was estimated using the Timur empirical relationship expressed in equation 7:

$$k = 0.136\phi^4 S_{wirr}^{-2} \quad (7)$$

where S_{wirr} is Irreducible water saturation and $\emptyset$ is porosity. These models offer a means to estimate permeability when core data is unavailable, though they should be calibrated with local data for accuracy (Asquith & Krygowski, 2004). These petrophysical parameters were used to evaluate reservoir quality and hydrocarbon saturation within the identified reservoir units. Seismic interpretation was then carried out on the 3D seismic dataset to define the structural framework of the field. Fault interpretation was performed by identifying reflector terminations, discontinuities, and abrupt offsets on seismic sections. The variance (coherency) attribute was generated to enhance the visibility of structural discontinuities and improve fault delineation (Umoren & George, 2018). Fault sticks were picked along multiple inlines and crosslines and subsequently interpolated to generate three-dimensional fault planes. Horizon interpretation was guided by well tops obtained from the well correlation and calibrated using seismic-to-well ties. The interpreted horizons corresponding to the reservoir units were mapped across the seismic volume to produce time-structure maps that reveal the structural configuration of the reservoirs. These time maps were converted to depth using velocity information derived from check-shot data.

To establish a reliable relationship between well data and seismic reflections, synthetic seismograms were generated using the convolutional model. Acoustic impedance was calculated from density and velocity logs using equation 8.

$$Z = \rho v \quad (8)$$

where Z represents acoustic impedance, ρ is density, and v is velocity. Reflection coefficients at layer interfaces were calculated using equation 9.

$$RC = \frac{Z_2 - Z_1}{Z_2 + Z_1} \quad (9)$$

where RC is the reflection coefficient, Z_1 is acoustic impedance in medium one and Z_2 is acoustic impedance in medium 2. This reflection coefficient is the ratio of change in acoustic impedance to twice the average in acoustic impedance across two boundaries. If Z_2 is greater than Z_1, then the reflection coefficient is positive. If Z_2 is less than Z_1, then the reflection coefficient is negative. After the reflection coefficient is calculated for all reflections in the seismic data, a seismic wavelet is extracted from the seismic traced at a surrounding the borehole. The synthetic seismogram was generated using equation 10.

$$x(t) = w(t) * RC \quad (10)$$

where $w(t)$is the seismic wavelet and RC represents the reflection coefficient series. The synthetic traces were matched with seismic traces at the well locations to achieve reliable

seismic-to-well ties and ensure accurate horizon picking.

Seismic attribute analysis was subsequently conducted to enhance the interpretation of reservoir geometry and potential hydrocarbon indicators (Ekefre et al., 2025). Both surface attributes and volume attributes were extracted from the seismic data. Surface attributes were computed along interpreted reservoir horizons to highlight variations in amplitude and structural geometry across the mapped surfaces. The key surface attributes generated include RMS amplitude, maximum amplitude, average amplitude, and surface variance (Ekanem et al., 2021b). RMS amplitude extracted along the reservoir horizons highlights zones of strong reflection energy that may indicate hydrocarbon-charged sand bodies. Surface variance attributes were used to delineate subtle structural discontinuities and fault patterns along the horizon surfaces.

Volume attributes were also computed throughout the seismic cube to enhance the detection of structural and stratigraphic features. RMS amplitude was calculated using equation 11, expressed as:

$$A_{RMS} = \sqrt{\frac{1}{N}\sum_{i=1}^{N} A_i^2} \qquad (11)$$

Instantaneous amplitude (envelope), which represents the total seismic energy at a given time, was calculated using equation 12, expressed as:

$$A_{inst} = \sqrt{S(t)^2 + H(t)^2} \qquad (12)$$

where $S(t)$is the seismic trace and $H(t)$is its Hilbert transform. Instantaneous frequency, which provides information about thin beds and stratigraphic variations, was obtained from the derivative of instantaneous phase shown in equation 13:

$$f(t) = \frac{1}{2\pi}\frac{d\phi(t)}{dt} \qquad (13)$$

Variance attributes were also generated to highlight reflector discontinuities associated with faults and fractures. The integration of these seismic attributes significantly enhanced the interpretation of structural closures, stratigraphic features, and amplitude anomalies within the field. Zones characterized by structural closure combined with strong amplitude anomalies were interpreted as potential hydrocarbon prospects.

Finally, volumetric estimation of hydrocarbons initially in place was carried out using parameters derived from structural mapping and petrophysical evaluation. Hydrocarbon initially in place (HIIP) was estimated using equation 14.

$$HIIP = GRV \times NTG \times \phi \times S_h \qquad (14)$$

Stock tank oil initially in place (STOIP) was calculated using the formula expressed in equation 15 while gas initially in place (GIIP) was estimated using 16.

$$STOIP = \frac{7758 \times GRV \times NTG \times \phi \times S_o}{B_o} \qquad (15)$$

$$GIIP = \frac{43560 \times GRV \times NTG \times \phi \times S_g}{B_g} \qquad (16)$$

where *GRV* represents gross rock volume, *NTG* is the net-to-gross ratio, ϕ is porosity, S_o and S_g are oil and gas saturations, respectively while B_o and B_g are the respective formation volume factors.

4.0 Results and Discussion

4.1 Well Correlation

Well correlation was carried out to establish the lateral continuity and stratigraphic relationships of hydrocarbon-bearing sand units across the X Field. The correlation utilized gamma ray (GR) and resistivity logs to distinguish sand from shale and identify potential hydrocarbon-bearing intervals. Gamma ray logs were used to delineate clean sand bodies and shale boundaries, while resistivity logs helped differentiate hydrocarbon-saturated zones from water-bearing formations (Akpan et al., 2021). The correlation was conducted along a west–east transect comprising six wells arranged in the sequence SAM-1, SAM-3, SAM-6, SAM-2, SAM-5, and SAM-4 (Figure 3). Two major sand bodies within the Agbada Formation were

identified and designated as Reservoir N and Reservoir O. Reservoir N represents the upper sand unit and is characterized by relatively low gamma ray values and high resistivity responses, indicating clean hydrocarbon-bearing sands. Reservoir O occurs below Reservoir N and shows a more serrated log pattern, reflecting interbedded sand–shale sequences typical of deltaic environments. Both reservoirs exhibit good lateral continuity across the wells, suggesting regionally extensive sand bodies deposited under relatively stable depositional conditions. Minor variations in thickness and resistivity responses across the wells indicate localized facies changes or subtle structural influences (George et al., 2010). The correlation confirms that Reservoirs N and O constitute the principal hydrocarbon-bearing units in the X Field, providing a stratigraphic framework for subsequent structural interpretation and seismic attribute analysis.

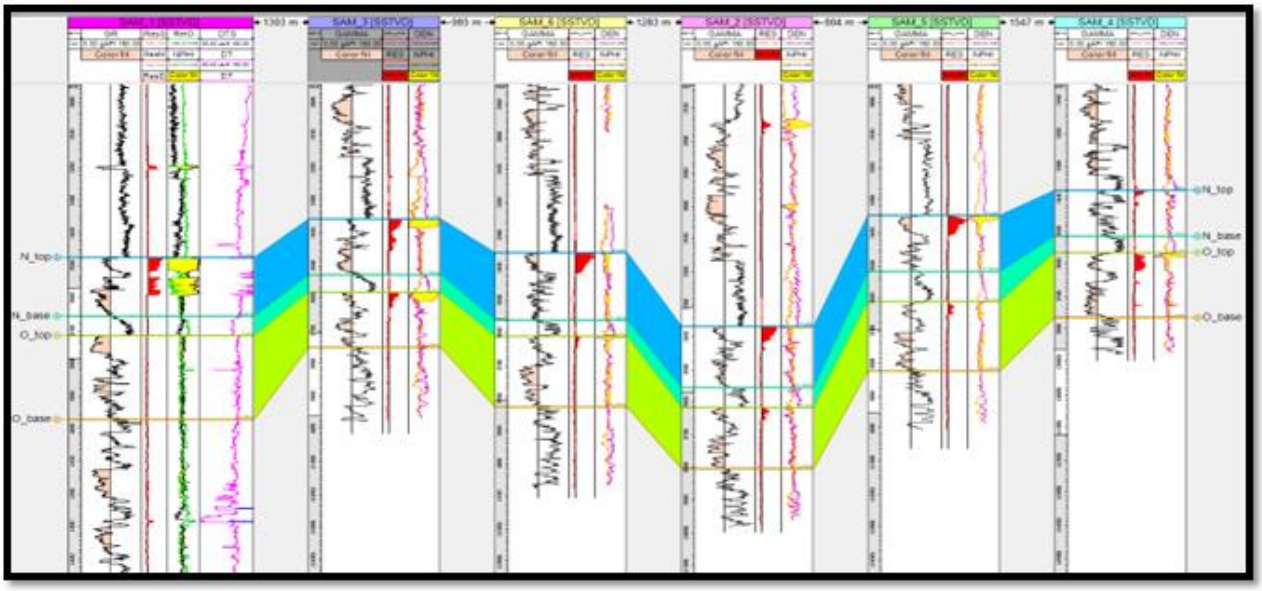

Figure 3: Well correlation panel showing Reservoirs N and O across wells in the X Field

4.2 Petrophysical Evaluation

Petrophysical analysis was carried out on six wells (SAM-1 to SAM-6) to evaluate the reservoir quality and hydrocarbon potential of Reservoirs N and O within the Agbada Formation. The key parameters analyzed include net-to-gross ratio (NTG), porosity (ϕ), and water saturation (Sw). The computed results are presented in Figures 4 and 5. For Reservoir N (Figure 4), NTG values ranged from 0.67 to 0.78 with an average of 0.74, indicating well-developed sand bodies with minimal shale intercalations. Porosity values vary between 0.22 and 0.28 (average ≈ 0.25), reflecting moderately good reservoir quality typical of Niger Delta sandstones. Water saturation ranged from 0.08 to 0.23 (average ≈ 0.15), suggesting high hydrocarbon saturation across the reservoir. For Reservoir O (Figure 5), NTG values ranged from 0.51 to 0.96 with an average of approximately 0.78, indicating good sand development with some degree of heterogeneity. Porosity values range from 0.21 to 0.27 (average ≈ 0.23), indicating moderately good reservoir quality comparable to Reservoir N. Water saturation varied between 0.00 and 0.30 (average ≈ 0.17), reflecting generally favorable hydrocarbon saturation with minor variations across the wells.

4.3 Synthetic Seismogram

The synthetic seismogram generated for SAM-1 was used to establish a seismic-to-well tie and validate the correlation between well log-derived reservoir tops and seismic reflections. The result (Figure 6) shows a good match between the synthetic and field seismic traces, indicating reliable data quality and an accurate

time-depth relationship. The major reflection events correspond closely with the tops of Reservoirs N and O, confirming that these units are well imaged within the seismic volume. Reflections associated with Reservoir N are relatively strong and continuous, suggesting good lateral continuity, whereas those of Reservoir O are comparatively less continuous, indicating minor lithologic variability (Ebong et al., 2021). The established tie provides confidence in the interpretation of reservoir horizons across the field.

4.4 Surface Attribute Analysis

Seismic attribute analysis revealed key structural, lithologic, and fluid-related characteristics of the X Field. The integration of multiple attributes enhances the delineation of reservoir geometry and hydrocarbon distribution within the Agbada Formation. The variance attribute (Figure 7) clearly delineates structural discontinuities within the field. High-variance zones define fault planes and fracture corridors, forming a network of synthetic and antithetic faults typical of the Niger Delta. These structures control reservoir compartmentalization and likely influence hydrocarbon migration pathways.

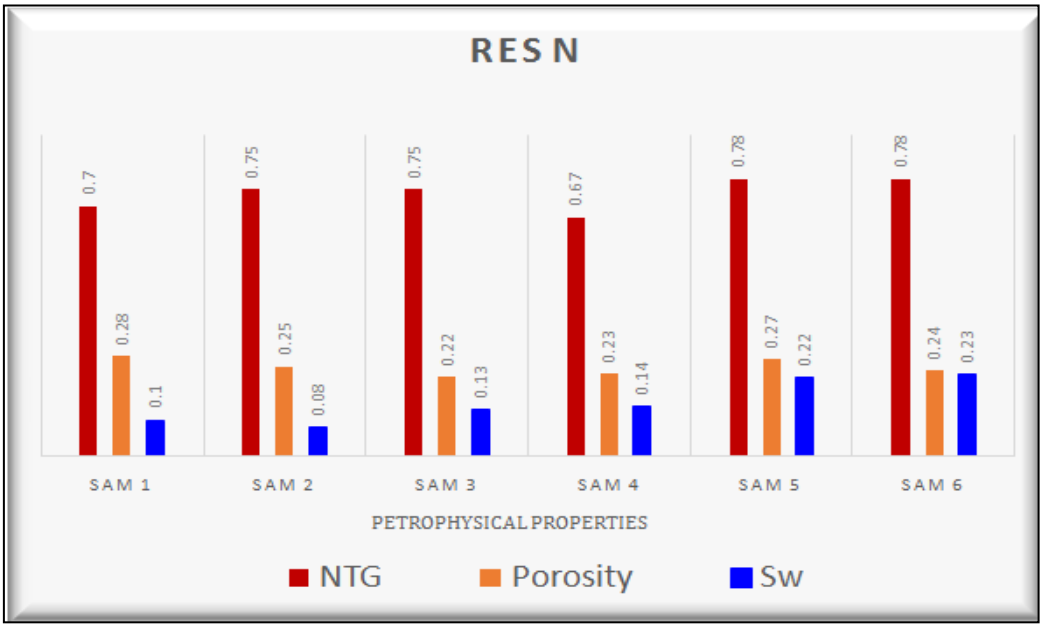

Figure 4: Comparative Petrophysical Plot for Reservoir N showing sand quality variation

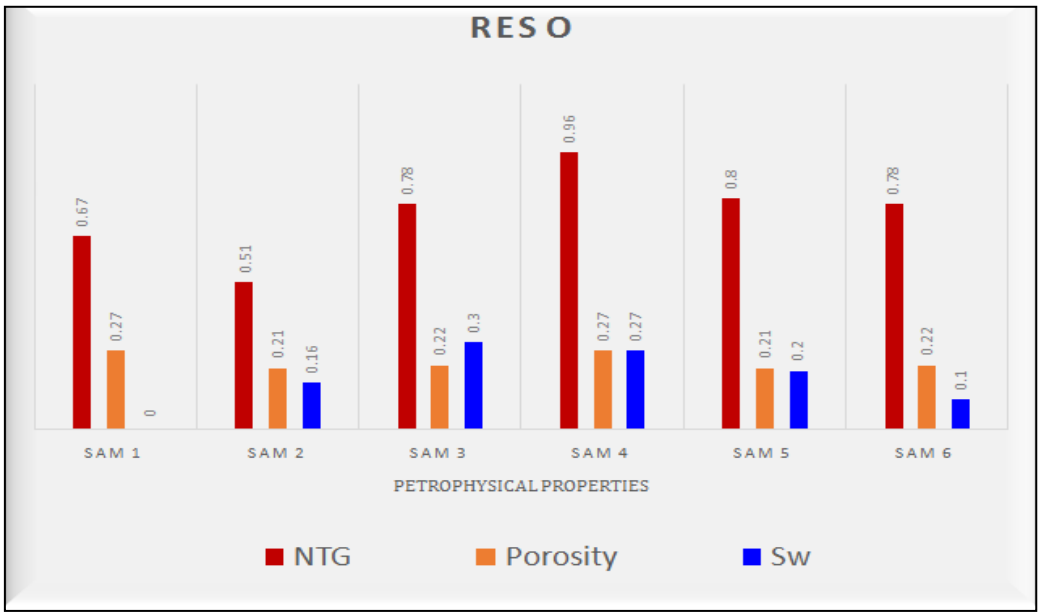

Figure 5: Comparative Petrophysical Plot for Reservoir O showing sand quality variation

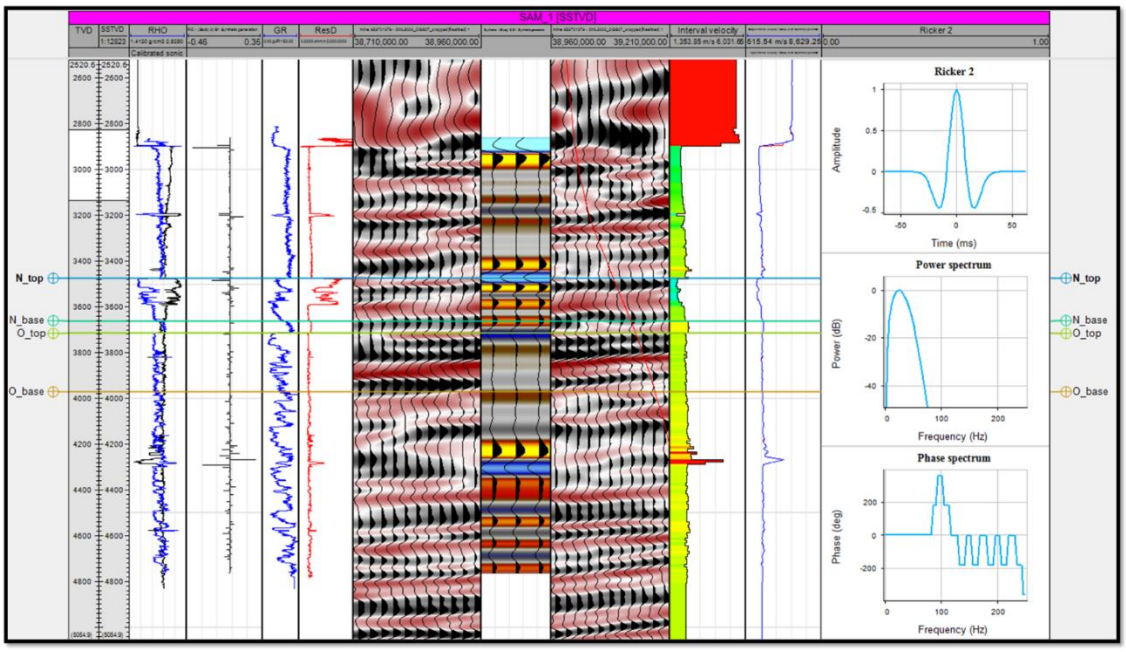

Figure 6: Synthetic seismogram showing seismic-to-well tie for SAM-1

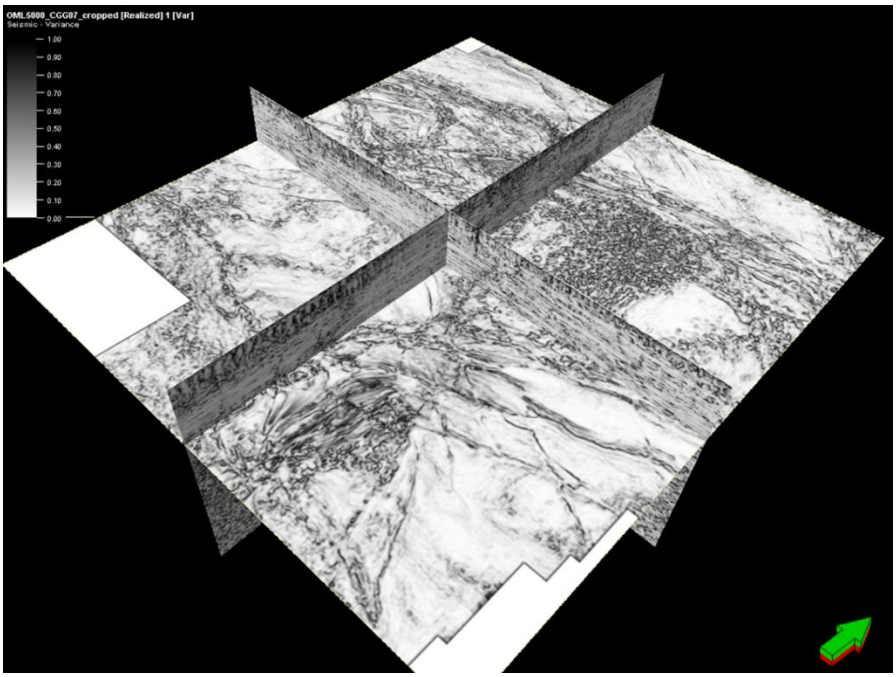

Figure 7: Variance attribute showing structural discontinuities and fault patterns

The Relative Acoustic Impedance (RAI) attribute (Figure 8) differentiates lithologic units within the field. Low-impedance zones correspond to porous sand bodies, while high-impedance zones indicate shale intervals. The low-impedance anomalies align with the mapped reservoir horizons and are concentrated within structural closures, suggesting hydrocarbon-bearing sands. The sweetness attribute (Figure 9) highlights zones of high amplitude and low frequency, which are indicative of hydrocarbon presence. High sweetness anomalies coincided with low-impedance regions and defined channel-like geometries, suggesting favorable reservoir distribution and continuity. The AVO fluid strength attribute (Figure 10) identifies fluid-related anomalies within the reservoir units. Positive AVO responses are observed in structurally elevated zones and correspond with previously identified amplitude anomalies, indicating hydrocarbon saturation within the sand bodies.

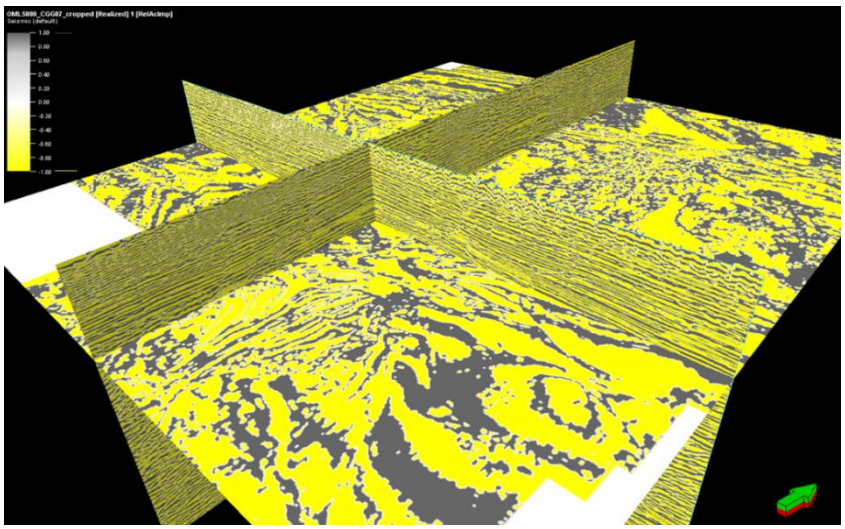

Figure 8: RAI attribute highlighting low-impedance reservoir zones

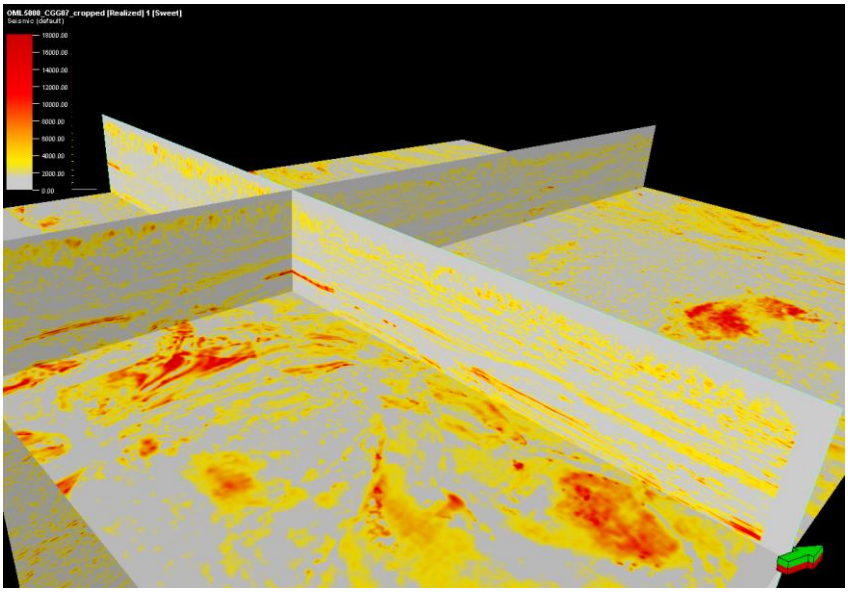

Figure 9: Sweetness attribute showing hydrocarbon-prone zones

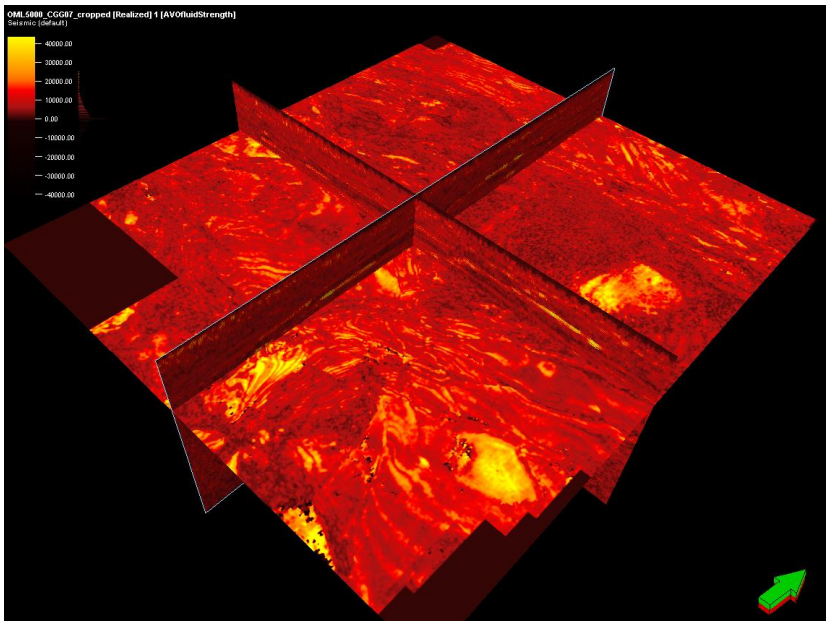

Figure 10: AVO fluid strength attribute highlighting hydrocarbon-bearing zones

The instantaneous phase attribute (Figure 11) enhances reflector continuity and structural definition. Continuous reflectors correspond to reservoir intervals, while phase discontinuities align with mapped faults and stratigraphic boundaries, confirming structural controls on reservoir distribution.

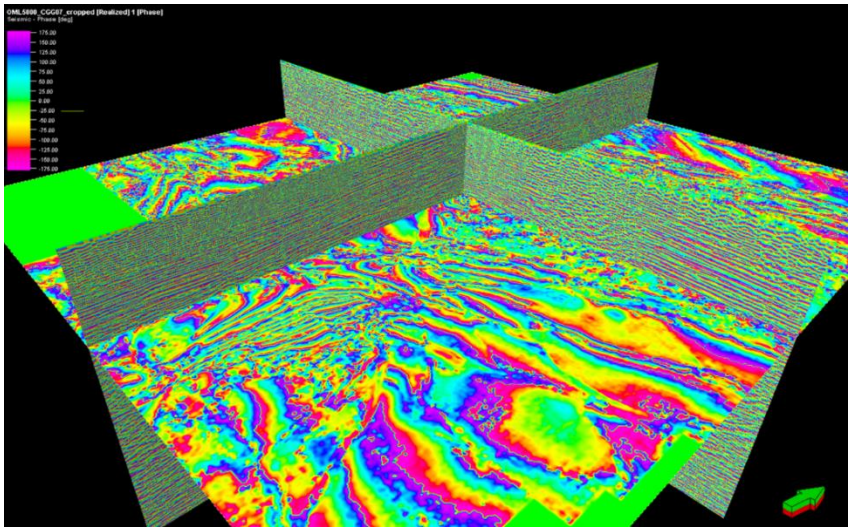

Figure 11: Instantaneous phase attribute showing reflector continuity and structural features

4.4 Structural Interpretation and Mapping

The structural framework (Figure 12) reveals a dominant Northwest–Southeast (NW–SE) trend, consistent with the regional extensional tectonic regime of the Niger Delta Basin. The major faults are elongate and subparallel, and are interpreted as listric normal faults that flatten with depth, reflecting gravity-driven deformation of the deltaic wedge and defining the structural architecture of the Agbada Formation. These anticlines constitute the principal structural traps, with hydrocarbons interpreted to migrate up-dip and accumulate within fault-bounded closures. Evidence of syn-depositional faulting is observed from the thickening of strata toward the fault planes, indicating strong structural control on sedimentation and reservoir development (Figure 12).

Fault interpretation was carried out to define the structural framework of the X Field and evaluate its influence on reservoir geometry and hydrocarbon distribution. Faults were identified on inline seismic sections as reflector discontinuities, offsets, and amplitude distortions. A total of thirty-five (35) faults were mapped across the seismic dataset (Figure 13), comprising major regional growth faults and smaller antithetic faults. The fault system segments the field into horst and graben blocks (Figure 13), with reservoir units forming rollover anticlines within the downthrown blocks of the major synthetic faults (Akpan et al., 2020).

Based on well-to-seismic correlation, two key horizons corresponding to Reservoirs N and O were interpreted across the seismic volume. These horizons represent the primary hydrocarbon-bearing intervals within the Agbada Formation and were mapped at 5 ms intervals to capture structural variability. The reflectors exhibit good lateral continuity, with localized disruptions at intersections with major NW–SE trending faults (Figure 14), indicating structural compartmentalization (Ebong et al., 2023). Reservoir N displays relatively smooth and continuous reflections, suggesting deposition under stable conditions and forming a laterally extensive sand body, whereas Reservoir O shows localized undulations and fault offsets, indicating greater structural deformation and possible facies variability.

Time structure maps generated for both reservoirs (Figure 15) delineate the subsurface configuration of the mapped horizons. Structural

highs define potential hydrocarbon closures, while structural lows indicate possible migration pathways or water-bearing zones. The contour patterns clearly reflect the influence of major and minor growth faults, with closures developed along fault-bounded anticlines, consistent with the regional structural style of the Niger Delta.

Depth structure maps were subsequently derived using a second-order polynomial velocity model (Figure 16), which provided a reliable time-to-depth conversion. The resulting depth maps (Figure 17) present the true structural geometry of the reservoirs, showing fault-bounded anticlinal closures as the principal trapping mechanisms. Reservoir N occurs at depths of approximately 3000–4800 ft, while Reservoir O lies deeper at about 3600–5400 ft. Variations in structural relief reflect differential compaction and fault-controlled deformation, with structural highs representing potential hydrocarbon-bearing zones and downthrown blocks indicating possible migration pathways or non-reservoir intervals.

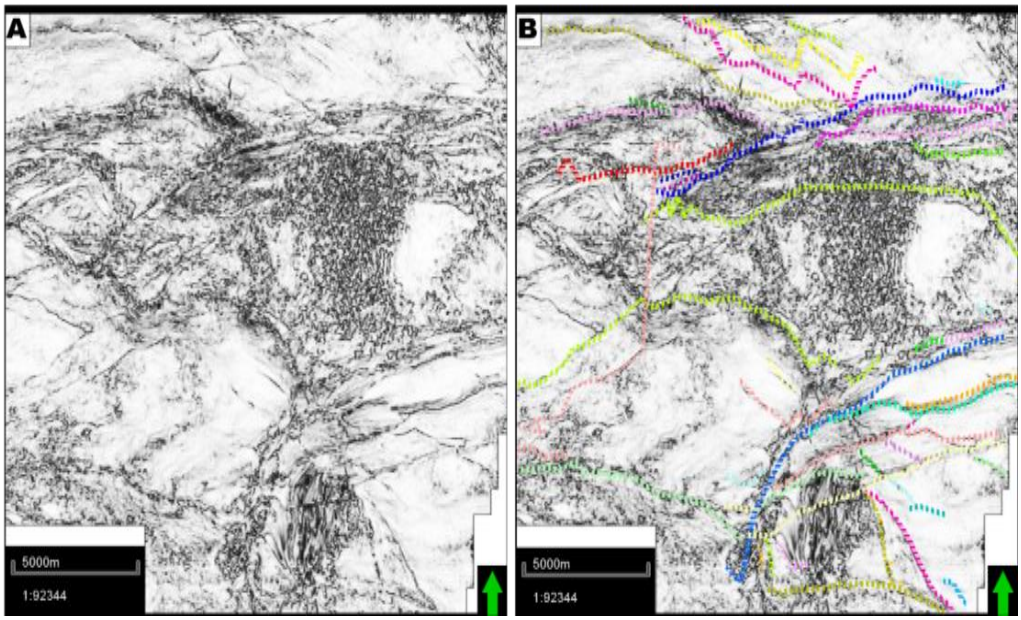

Figure 12: Variance attribute time slice showing uninterpreted (A) and interpreted (B) discontinuities

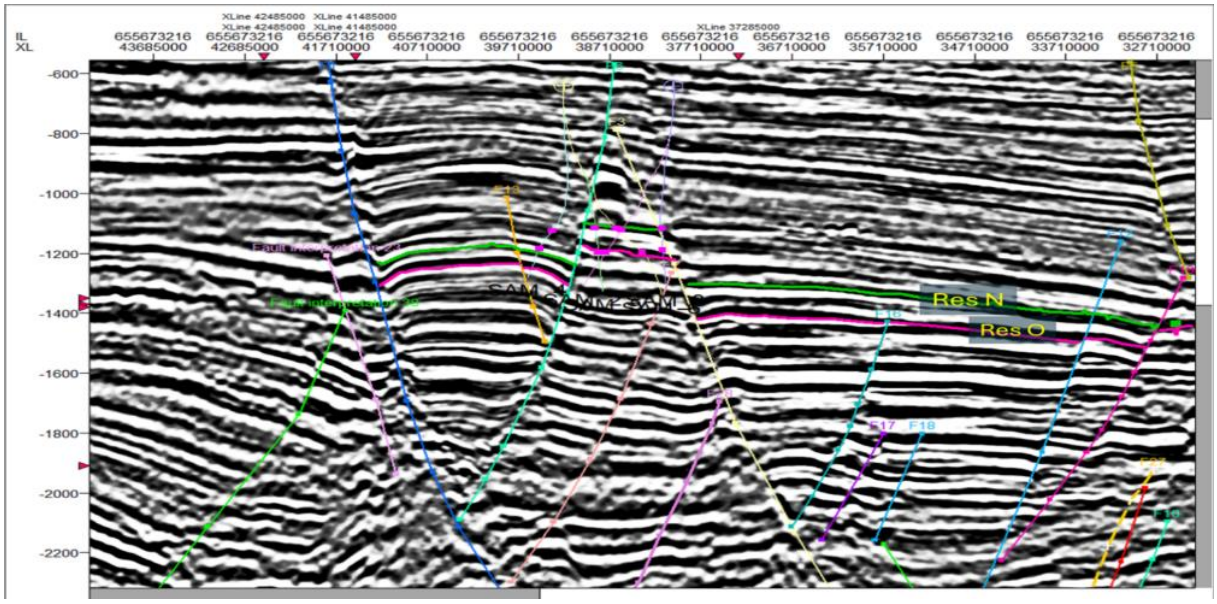

Figure 13: Interpreted faults and horizons on seismic inline

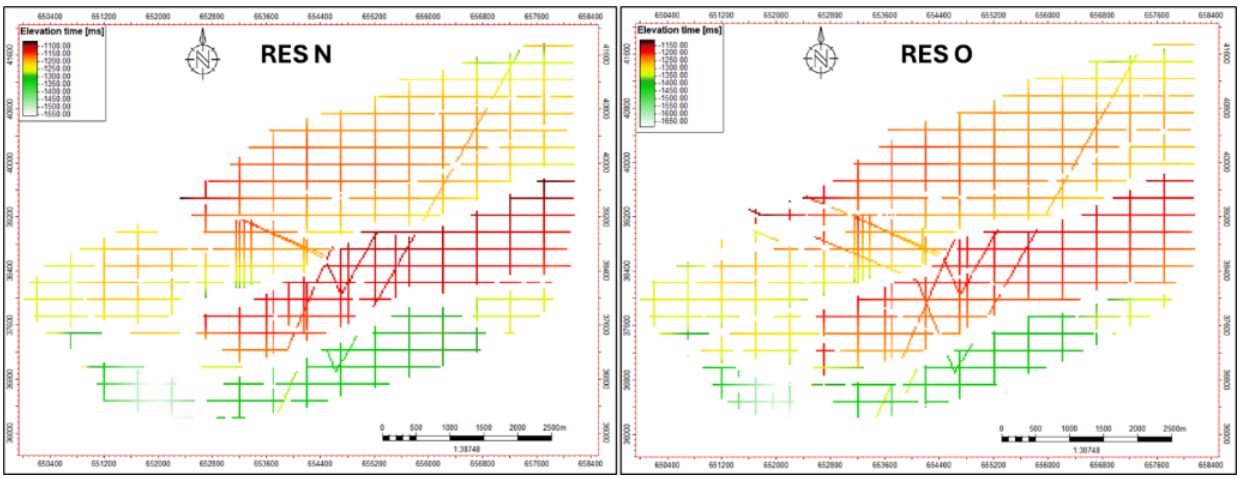

Figure 14: Interpreted horizons for Reservoirs N and O

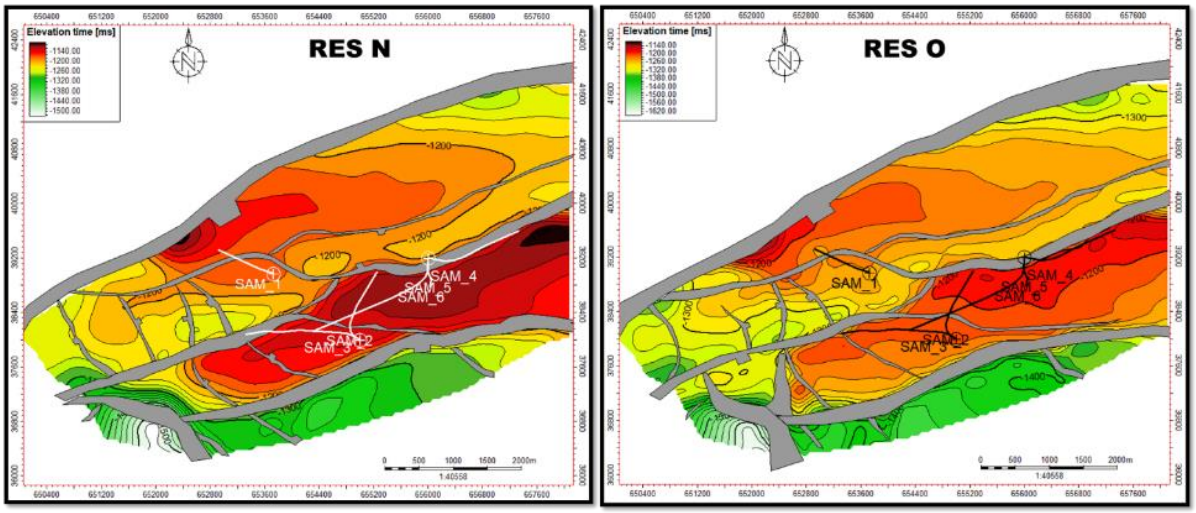

Figure 15: Time structure maps for Reservoirs N and O

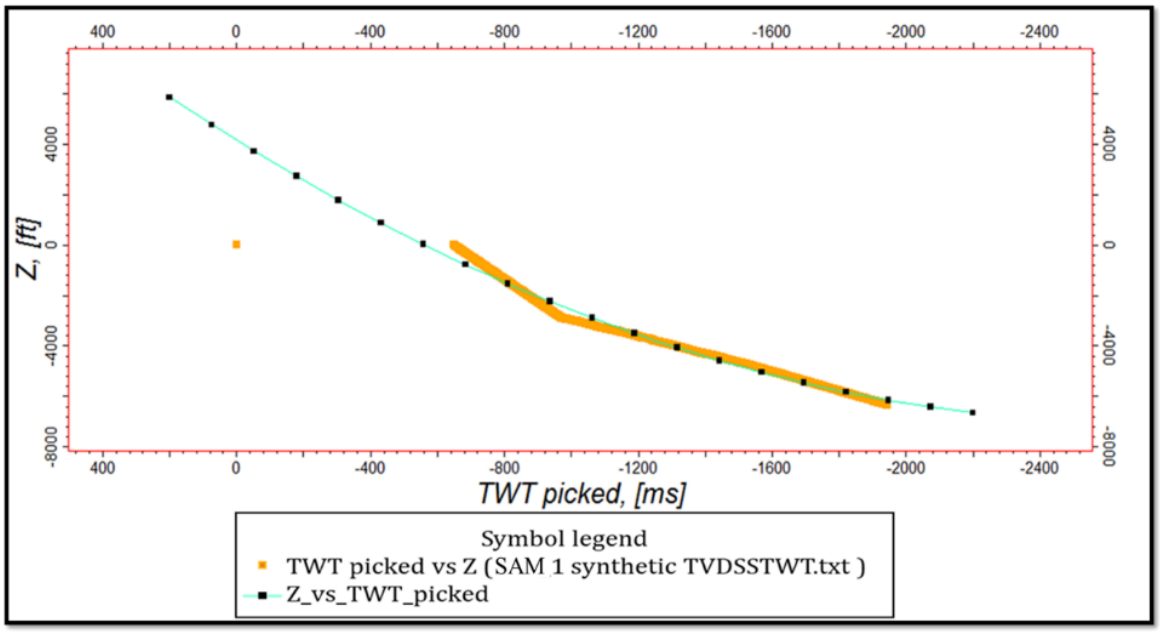

Figure 16: Velocity model for time–depth conversion

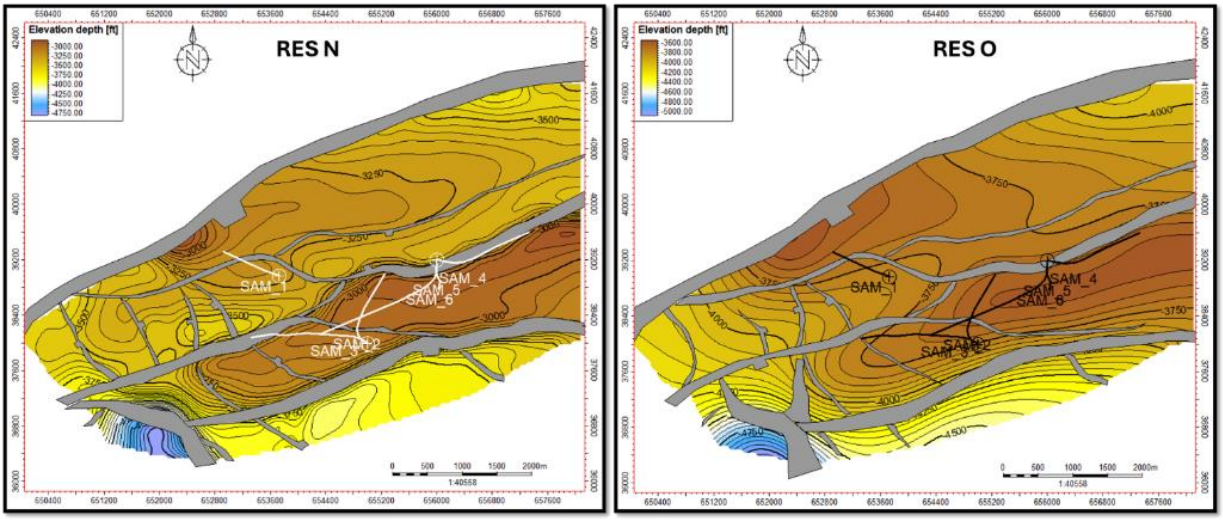

Figure 17: Depth structure maps for Reservoirs N and O

4.5 Surface Attribute Analysis and Prospect Identification

Surface seismic attributes extracted from the mapped time surfaces of Reservoir N and Reservoir O provide a clear lateral expression of seismic response, enabling improved delineation of structural configuration, lithologic variation, and hydrocarbon distribution across the field. The combined analysis of RMS amplitude, maximum amplitude, maximum magnitude, sum of amplitudes, and sum of magnitudes reveals consistent spatial patterns that are strongly controlled by the structural framework.

The RMS amplitude maps (Figure 18 a & b) display prominent high-amplitude anomalies trending northwest–southeast, which coincide with the crestal regions of rollover anticlines. These amplitude highs are spatially aligned with fault-bounded closures and are interpreted as zones of increased reflection energy associated with hydrocarbon-bearing sands. Conversely, low RMS amplitude values occur within structurally low areas and downthrown fault blocks, suggesting shale-prone or water-bearing intervals. This distribution highlights the effectiveness of RMS amplitude in delineating prospective zones along structural highs. The concentration of high RMS amplitude anomalies along structurally elevated rollover anticlines suggests enhanced hydrocarbon charge and preservation within fault-bounded closures. This observation is consistent with the established petroleum system architecture of the Niger Delta, where listric growth faults provide migration pathways while simultaneously acting as lateral seals (Doust & Omatsola, 1990). The amplitude enhancement likely reflects strong impedance contrasts associated with hydrocarbon-filled porous sandstones.

Similarly, the maximum amplitude attribute (Figure 19a & b) identifies localized bright spots concentrated around updip closures, particularly along the western structural crests. These amplitude maxima indicate strong impedance contrasts typically associated with hydrocarbon saturation. The correspondence between amplitude highs and structural culminations further confirms that hydrocarbon accumulation is structurally controlled, while localized amplitude dimming along fault zones may indicate lithologic variation or minor leakage pathways.

The maximum magnitude attribute maps (Figure 20a & b) provide additional insight into the distribution of reflection energy within Reservoirs N and O by emphasizing zones characterized by strong seismic responses. The concentration of high-magnitude anomalies along the crestal portions of the mapped rollover anticlines suggests that these structurally elevated regions contain significant acoustic impedance contrasts, which are commonly associated with hydrocarbon-charged sand bodies.

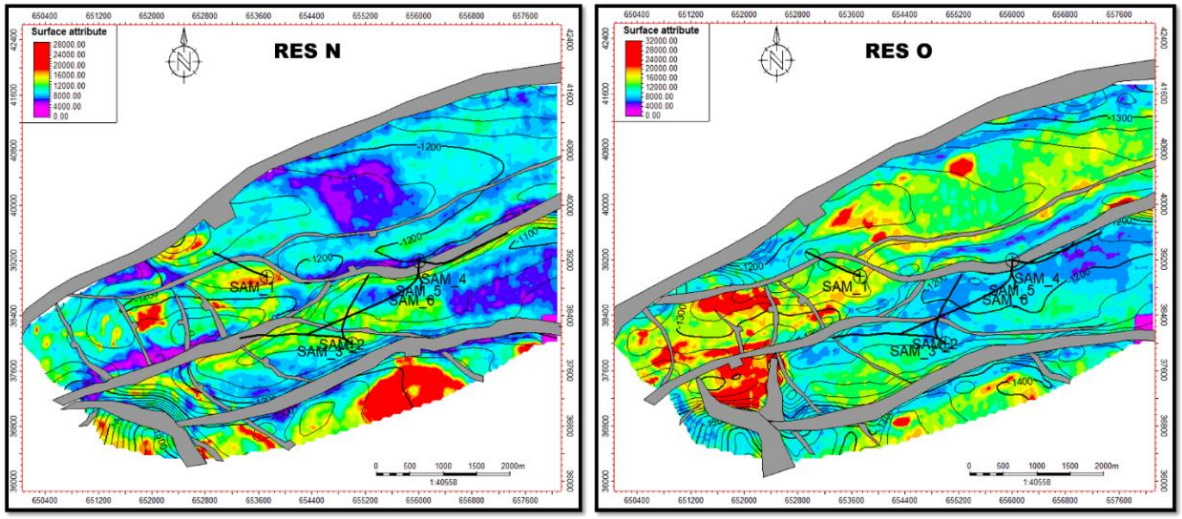

Figure 18: RMS Amplitude surface maps for Reservoir N (a) and Reservoir O (b) showing amplitude highs corresponding to fault-bounded structural closures

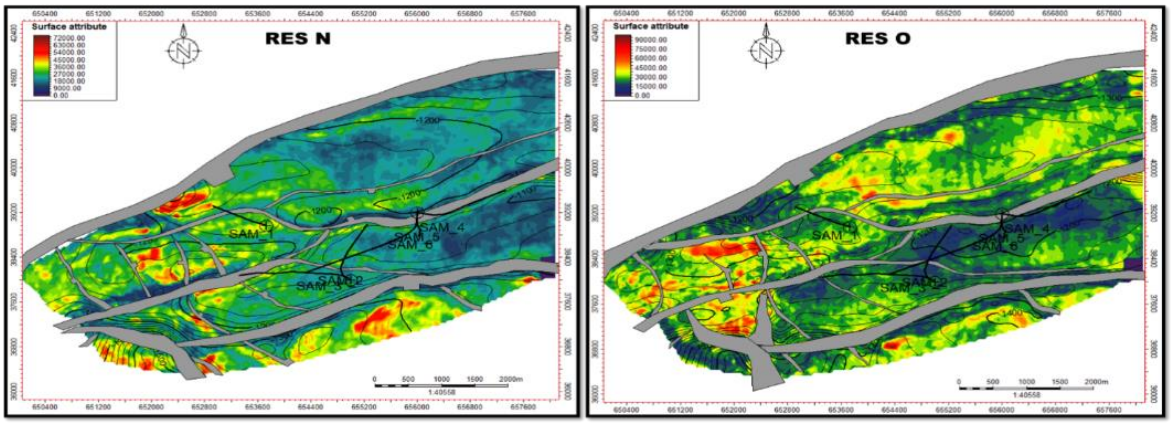

Figure 19: Maximum Amplitude attribute maps for Reservoir N (a) and Reservoir O (b) showing amplitude maxima over structural crests and closure boundaries

The close spatial relationship between the maximum magnitude highs and the structural culminations confirms that the rollover anticlines constitute the principal trapping mechanisms within the field. This observation is consistent with the structural style of the Niger Delta, where listric growth faults generate fault-assisted anticlines that facilitate hydrocarbon migration and accumulation within structurally favorable closures (de la Barra et al., 2024)

Furthermore, the persistence of these high-magnitude responses across both reservoirs indicates lateral continuity of the reservoir sands and suggests that hydrocarbon saturation is not localized to isolated pockets but extends across structurally connected zones. The enhanced reflection intensity observed at these crestal regions may also reflect improved reservoir quality, including cleaner sands, better porosity development, and stronger fluid effects resulting from hydrocarbon emplacement. The alignment of these anomalies with previously identified RMS amplitude and maximum amplitude highs further strengthens the interpretation of productive reservoir intervals within the field (Navarro-Perez et al., 2025).

Conversely, the relatively low-magnitude responses observed within the downthrown fault blocks likely indicate less favorable reservoir conditions. These subdued reflections may result from increased shale intercalation, greater compaction at structurally lower positions, or reduced hydrocarbon saturation. In deltaic depositional environments such as the Niger Delta, downthrown blocks commonly experience thicker shale accumulation and

differential compaction, which can reduce porosity and weaken impedance contrasts. In some areas, the diminished seismic magnitude may also suggest water-bearing intervals or poor reservoir connectivity due to fault compartmentalization (Lin et al., 2025). Therefore, the contrast between the high-magnitude structural crests and the lower-magnitude downthrown zones highlights the strong structural control on reservoir development, hydrocarbon distribution, and trap effectiveness within the X Field.

The sum of amplitudes maps (Figure 21a & b) reveals laterally continuous, high-energy reflection trends oriented parallel to the dominant northwest–southeast fault system. These trends correspond to thicker, stacked sand bodies, indicating amalgamated channel deposits and enhanced reservoir development. The concentration of amplitude summation peaks along structural highs further supports the interpretation of hydrocarbon accumulation within fault-bounded closures, while also suggesting good lateral reservoir connectivity.

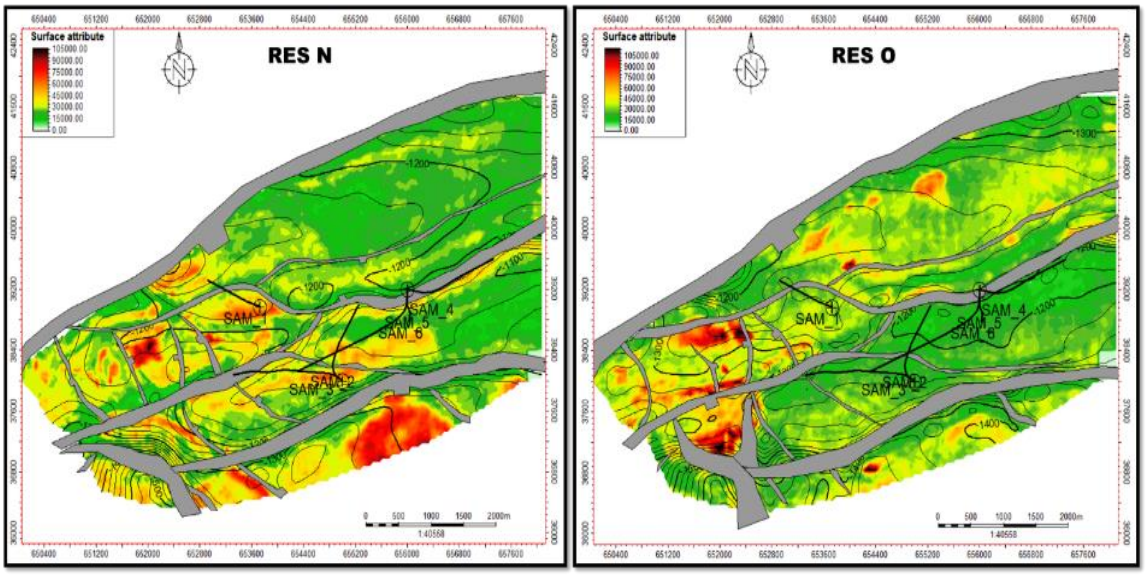

Figure 20: Maximum Magnitude maps for Reservoir N (a) and Reservoir O (b), highlighting high-magnitude zones along the structural crests, indicative of potential hydrocarbon charge

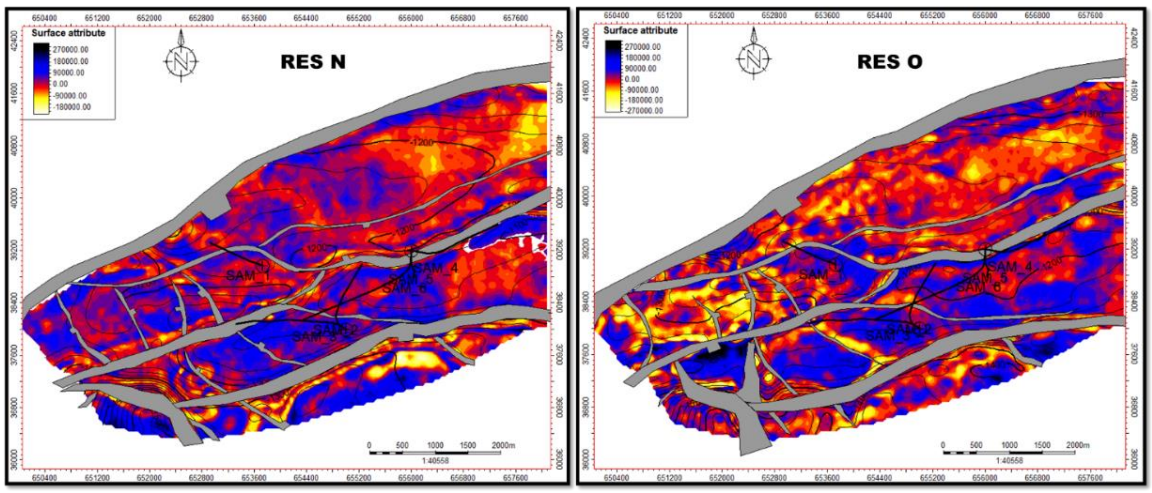

Figure 21: Sum of Amplitudes maps for Reservoir N (a) and Reservoir O (b) illustrating laterally continuous high-amplitude zones corresponding to potential sand body development

The sum of magnitudes attribute (Figures 22a and 22b) provides important insight into the spatial distribution of reflection energy and its relationship with structural trapping within the reservoirs. The attribute reveals laterally continuous zones of high reflection intensity that

are concentrated mainly along structurally elevated regions and bounded by major growth faults. These high-magnitude anomalies are interpreted as areas of enhanced reservoir development characterized by thicker sand accumulations and significant acoustic impedance contrasts between hydrocarbon-filled sands and surrounding shale units (Asif et al., 2024). The strong reflectivity observed within these zones suggests the presence of porous and hydrocarbon-saturated sandstone bodies, which are typical of productive Agbada Formation reservoirs in the Niger Delta.

A notable feature of the attribute response is the abrupt termination of the high-magnitude trends against the mapped fault planes. This truncation pattern indicates that the faults are not merely structural discontinuities but are likely acting as effective sealing barriers that restrict lateral hydrocarbon migration. Such sealing behavior promotes the accumulation and preservation of hydrocarbons within discrete fault-bounded compartments. The compartmentalized nature of the reservoirs implies that hydrocarbon distribution within the field is strongly controlled by the geometry and sealing capacity of the growth fault system (Gao et al., 2025).

Furthermore, the alignment of the high-magnitude anomalies with rollover anticline crests suggests that structural deformation played a major role in creating accommodation space for sediment deposition and subsequent hydrocarbon entrapment. The combination of structural closure, enhanced sand development, and strong seismic response therefore supports the interpretation that these zones represent the most prospective hydrocarbon-bearing intervals within the field. This observation is consistent with the established petroleum system of the Niger Delta, where listric growth faults commonly function as migration pathways during hydrocarbon charging and later serve as sealing mechanisms that localize hydrocarbon accumulation within rollover anticline traps.

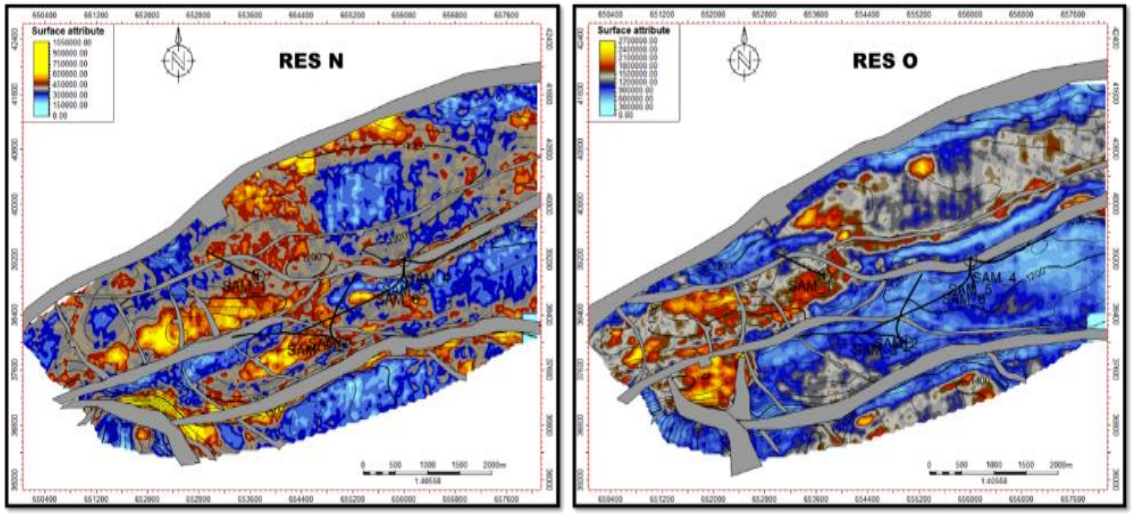

Figure 22: Sum of Magnitudes maps for Reservoir N (a) and Reservoir O (b) showing high-intensity reflection zones bounded by growth faults, indicating fault-controlled hydrocarbon entrapment

The integration of all surface attributes reveals a consistent pattern of amplitude and magnitude enhancement concentrated along structural highs and rollover anticlines. High RMS amplitude, maximum amplitude, and maximum magnitude responses coincide with crestal closures, indicating fluid saturation effects, while the sum-based attributes delineate thicker and laterally continuous sand bodies within these closures. These combined observations confirm that hydrocarbon accumulation in the X Field is primarily structurally controlled, with migration pathways terminating against sealing fault planes. Based on this integrated attribute analysis, five fault-bounded prospects (A–E) were identified within Reservoir N (Figure 23), while four additional prospects (F–I) were delineated within Reservoir O (Figure 24).

These prospects correspond to zones where structural closure, amplitude anomalies, and reservoir continuity converge, representing the most promising targets for hydrocarbon exploration and development within the field.

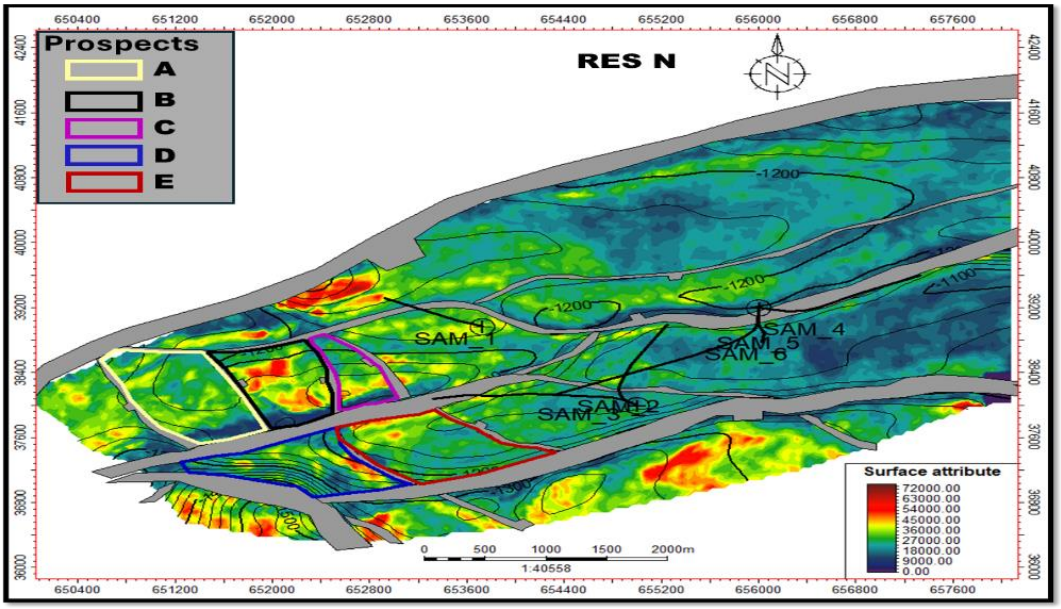

Figure 23: Integrated surface attribute overlay for Reservoir N showing combined high-response zones that define structurally controlled hydrocarbon prospects (A -E)

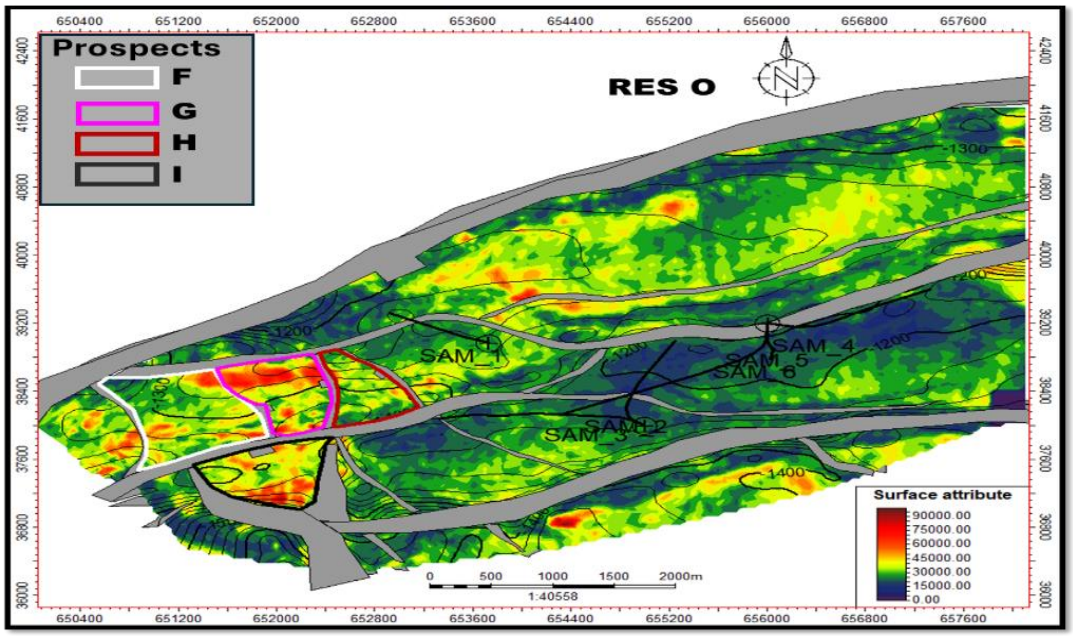

Figure 24: Integrated surface attribute overlay for Reservoir O showing combined high-response zones that define structurally controlled hydrocarbon prospects (F - I)

4.6 Volumetric Estimation

Volumetric estimation was carried out to determine the Hydrocarbons Initially in Place (HIIP) for the mapped prospects in the X Field using petrophysical parameters derived from well log interpretation and structural inputs from seismic mapping. This analysis provides a quantitative evaluation of the hydrocarbon potential of each identified prospect within the two principal reservoir units (Reservoir N and Reservoir O) of the Agbada Formation in the Niger Delta Basin. The calculations were based on standard deterministic volumetric equations (Archie, 1942; Tiab & Donaldson, 2015),

incorporating Gross Rock Volume (GRV), Net-to-Gross ratio (NTG), average porosity (ϕ), water saturation (Sw), and formation volume factors (Boi and Bgi). The results (Table 1) indicate notable variations in hydrocarbon volumes across the mapped prospects reflect differences in structural geometry, reservoir quality, and trap efficiency.

Table 1: Volumetric results for the prospects across RES N and RES O

PROSPECT	AREA (acre)	OIL GRV (acre.ft)	GAS GRV (acre.ft)	GRV (acre.ft)	Av.NTG (frac)	Av. PHI (frac)	Av. Sw (frac)	Boi	Bgi	STOIIP (MMBOE)	GIIP (MSCF)	HIIP (MMBOE)
A	231.71	6410.70	12164.88	18575.58	0.79	0.25	0.15	1.25	0.8	1178700.55	19622939.84	20801640.38
B	167.90	4645.34	8814.96	13460.30	0.79	0.25	0.15	1.25	0.8	854114.32	14219246.70	15073361.01
C	77.62	2147.44	4074.96	6222.40	0.79	0.25	0.15	1.25	0.8	394838.13	6573242.78	6968080.91
D	180.86	5003.79	9495.15	14498.94	0.79	0.25	0.15	1.25	0.8	920020.46	15316448.43	16236468.89
E	214.03	5921.47	11236.52	17157.99	0.79	0.25	0.15	1.25	0.8	1088748.53	18125423.76	19214172.29
F	222.58	4260.82	7154.36	11415.17	0.78	0.23	0.17	1.25	0.8	806499.34	11880640.66	12687140.00
G	139.51	2670.52	4484.09	7154.61	0.78	0.23	0.17	1.25	0.8	505484.28	7446350.86	7951835.14
H	96.88	1854.63	3114.12	4968.75	0.78	0.23	0.17	1.25	0.8	351050.05	5171361.37	5522411.42
I	146.70	2808.22	4715.29	7523.51	0.78	0.23	0.17	1.25	0.8	531547.49	7830291.23	8361838.73

Reservoir N comprises five fault-bounded structural closures (Prospects A - E) and represents the most hydrocarbon-rich interval in the field (Akpan et al., 2022). The GRV values range from approximately 6,222.40 acre.ft in Prospect C to 18,575.58 acre.ft in Prospect A, indicating variability in trap size and structural closure. Prospect A is the most significant accumulation, with an estimated HIIP of about 20.8 MMBOE, supported by its large GRV, high NTG (0.79), and moderate porosity (0.25). Prospects E and D also show substantial hydrocarbon volumes of approximately 19.2 MMBOE and 16.2 MMBOE, respectively, while Prospect B contributes about 15.1 MMBOE. Prospect C, although the smallest structure, still contains a moderate hydrocarbon volume of approximately 6.97 MMBOE, suggesting that reservoir continuity extends across the field despite structural segmentation. The cumulative HIIP for Reservoir N is approximately 78.29 MMBOE, with GIIP values exceeding 73.8 BSCF, indicating that this reservoir hosts the majority of the field's hydrocarbon resources. The consistently high NTG (≈0.79), moderate porosity (≈0.25), and low water saturation (≈0.15) suggest well-sorted, clean sandstones with excellent storage capacity and connectivity. These hydrocarbons are structurally trapped within rollover anticlines bounded by listric growth faults, consistent with the Niger Delta petroleum system.

Reservoir O, which occurs at greater depths, contains four mapped prospects (F–I) with GRV values ranging from approximately 4,968.75 acre.ft to 11,415.17 acre.ft. Prospect F is the most significant in this interval, with an estimated HIIP of about 12.6 MMBOE, making it the primary target within the deeper reservoir. Prospects G and I exhibit moderate hydrocarbon volumes of approximately 7.95 MMBOE and 8.36 MMBOE, respectively, while Prospect H, though the smallest, still contains about 5.52 MMBOE. The total HIIP for Reservoir O is estimated at approximately 34.5 MMBOE, with a cumulative GIIP of about 32.5 BSCF. Compared to Reservoir N, Reservoir O shows slightly reduced reservoir quality, with lower porosity (≈0.23) and higher water saturation (≈0.17), reflecting compaction effects associated with greater burial depth. However, the high NTG (≈0.78) indicates that sand bodies remain thick and laterally continuous. Hydrocarbon accumulation in this reservoir is also structurally controlled, with fluids localized within fault-bounded anticlines and rollover structures.

An integrated assessment of both reservoirs indicates that the X Field contains a total HIIP of approximately 112.81 MMBOE, with Reservoir N contributing about 69% (≈78.29 MMBOE)

and Reservoir O contributing about 31% (≈34.52 MMBOE). This distribution confirms that Reservoir N is the dominant production target, while Reservoir O provides additional exploration potential. The high NTG and consistent porosity values across both reservoirs indicate a well-connected depositional system composed of laterally extensive sandstone bodies typical of the Agbada Formation (Doust and Omatsola, 1990). Structurally, hydrocarbon accumulation is governed by fault-controlled rollover anticline traps, where listric growth faults act as both migration pathways and sealing barriers. The vertical distribution of hydrocarbons further suggests a segregated system, with gas predominating in the shallower Reservoir N and oil more dominant in the deeper Reservoir O, consistent with buoyancy-driven migration and trapping mechanisms in the Niger Delta (Evamy et al., 1978).

5.0 Summary, conclusion and recommendations

This study presents an integrated geophysical and petrophysical evaluation of the X Field in the Niger Delta Basin, combining well log analysis with 3D seismic interpretation to characterize reservoir properties, structural controls, and hydrocarbon potential within the Agbada Formation. Two main reservoirs, Reservoir N and Reservoir O, were identified across six wells, both exhibiting good reservoir quality with high net-to-gross ratios, moderate to high porosity, and low to moderate water saturation. Reservoir N shows slightly better reservoir characteristics, while Reservoir O remains a viable secondary target despite deeper burial and compaction effects. Structural interpretation reveals that hydrocarbon accumulation in the field is primarily controlled by listric growth faults and associated rollover anticlines, which act as both migration pathways and trapping mechanisms. Seismic attribute analysis further confirms this, with amplitude anomalies and low-impedance zones aligning with structural highs and fault-bounded closures, indicating hydrocarbon presence and reservoir continuity. Volumetric estimation indicates a total Hydrocarbons Initially in Place (HIIP) of approximately 112.81 MMBOE, with Reservoir N contributing about 78.29 MMBOE and Reservoir O about 34.52 MMBOE. The most promising prospects are A, E, and D in Reservoir N, while F and I in Reservoir O offer additional development potential. These results confirm that hydrocarbon distribution is strongly structurally controlled and concentrated within rollover anticline crests.

In conclusion, the X Field represents a structurally controlled, multi-reservoir hydrocarbon system with significant commercial potential. The consistency between petrophysical properties, seismic attributes, and volumetric results validates the integrated workflow adopted in this study and aligns with established models of hydrocarbon accumulation in the Niger Delta. To enhance field development, drilling should prioritize the most prospective closures (A, E, and D), while advanced seismic inversion, fault seal analysis, and reservoir modeling are recommended to reduce uncertainty and optimize recovery. Further integration of geomechanical studies and advanced analytical techniques will improve reservoir management and long-term production performance. Finally, this study demonstrates that a well-integrated seismic–petrophysical approach remains critical for accurately characterizing reservoirs and unlocking hydrocarbon potential in complex deltaic environments such as the Niger Delta.

References

Akpan, A.S., Obiora, D.N., Okeke, F.N., Ibuot, J.C., George, N.J. (2020). Influence of wavelet phase rotation on post stack model based seismic inversion: A case study of X-field, Niger Delta, Nigeria, *Journal of Petroleum and Gas Engineering*, Vol.11(1), pp. 57-67, January 2020, https://doi.org/10.58-97/JPGE2019.0320

Akpan, A.S., Okeke, F.N., Obiora, D.N. George, N.J. (2021). Modelling and mapping hydrocarbon saturated sand reservoir using Poisson's impedance (PI) inversion: a case study of Bonna field, Niger Delta swamp depobelt, Nigeria. *J Petrol Explor Prod Technol* **11**, 117–132 (2021). https://doi.org/10.1007/s13202-020-01027-8

Akpan, M.J., George, N.J., Ekanem, A.M. & Ekong, U.N. (2022). Petrophysical appraisal and 3-D structural interpretation of reservoirs in an Onshore Niger Delta Field, Southeastern Nigeria. *Int J Energy Water Res.,* 9, 89–101 (2025). https://doi.org/10.1007/s42108-022-00218-9.

Archie, G. E. (1942). The electrical resistivity log as an aid in determining some reservoir characteristics. *Transactions of the AIME*, 146(1), 54–62.

Asif, M., Anjum, M. N., Azam, M., Hussain, F., Afzal, A., Kim, B. S., Maeng, S. J., Kim, D., & Iqbal, W. (2024). Climate-Driven Changes in the Projected Annual and Seasonal Precipitation over the Northern Highlands of Pakistan. *Water*, *16*(23), 3461. https://doi.org/10.3390/w162334-61

Asquith, G. B., & Krygowski, D. (2004). Basic Well Log Analysis (2nd ed.). AAPG Methods in Exploration Series No. 16.

Atat J.G., Akpabio I.O., George, N.J. (2013). Allowable Bearing Capacity for Shallow Foundation in Eket Local Government Area, Akwa Ibom State, Southern Nigeria. *International Journal of Geosciences*, 4(10), 1491-5000

Attai, E. S., Ebong, S.T. & Joshua, E. O. (2015). Application of Vertical Electrical Sounding to Investigate the Groundwater Potential in Abak Local Government Area, Akwa Ibom State, Nigeria. *Journal of Geography, Environment and Earth Science, 5(12), 43–57.*

Attai, E. S; Akpabio, G. T; Atat, J.G and Ebong, S.T (2025): Sandstones reservoir quality of central Niger delta basin from petrophysical parameters account using well log data. *World Journal of Advanced Science and Technology, 2025, 08(01), 001-011.* Article DOI: https://doi.org/10.53346/wjast.2025.8.1.0020.

Barnes, A. E., (2016), A filter to improve seismic discontinuity data for fault interpretation: *Geophysics*, 71, P1–P4.

Brown, A. R. (2011). Interpretation of Three-Dimensional Seismic Data (7th ed.). AAPG Memoir 42, SEG Investigations in Geophysics No. 9.

Chopra, S., & Marfurt, K.J., (2007). Seismic Attributes for Prospect Identification and Reservoir Characterization (Geophysical Developments Series 11). Society of Exploration Geophysicists, USA.

de la Barra, E., Vega-Jorquera, P., & da Silva, S. L. E. F. (2024). Multimodal Non-Extensive Frequency-Magnitude Distributions and Their Relationship to Multi-Source Seismicity. *Entropy*, *26*(12), 1040. https://doi.org/10.3390/e261210-40.

Doust, H., & Omatsola, E. (1990): Niger Delta, *in*, Edwards, J. D., and Santogrossi, P.A., eds., Divergent/passive Margin Basins, AAPG Memoir 48: Tulsa, American Association of Petroleum Geologists, p. 239-248. *Earth Science International, 3(1): 1-12, 2015; Article no. JGEESI.17832.,* SCIENCEDOMAIN *international www.sciencedomain.org*

Ebong S. T., Joshua, E. O., Ekong U. N., &. Akpabio, G. T. (2020). Reservoir Properties Discrimination in Soku field, Niger Delta, Using cross plotting Techniques. *IOSR Journal of Applied Physics (IOSR-JAP)* e-ISSN: 2278-4861.Volume 12, Issue 3 Ser. IV (May – June 2020), PP 19-32 www.Iosrjournals.Org

Ebong, S. T; Ekong, U. N.; Joshua, E. O; Akpabio, G.T; Efiang, J.A; Attai, E. S. & Ekanem, K. R (2021): Rock Attributes for Reservoir Discrimination Using Lame's Parameters. Quest Journals: *Journal of Research in Environmental and Earth Sciences* Volume 7 ~ Issue 7 (2021) pp: 12-32 ISSN(Online) :2348-2532 www.questjournals.org

Ebong, S. T. Ekanem, A.M. & George, N.J. (2023). Reservoir Characterisation Using Seismic Inversion Techniques for Mapping of Prospects, *Researchers Journal of Science and Technology (2023) 3(1): 1 – 13.*

Ebong, S. T., Ekanem, A. M. & George, N. J. (2023). Fluid Prediction Through Lithological Analysis in 'M' Oil Field Niger Delta: Using Rock Physics Approach. *Earth Sciences Malaysia, 7(1): 55 - 61.*

Ekanem, A. M. & Ebong, S. T. (2025). Combined geophysical and hydrogeological evaluation of groundwater characteristics in and around Obio Akpa Campus, Akwa Ibom State University, Nigeria. *Discover Geoscience* (2025) 3:188. https://doi.org/10.1007/s44-288-025-00309-0.

Ekanem, A. M. & Ebong, S. T. (2026). Geophysical and hydrogeochemical assessments of groundwater quality conditions for domestic and irrigation purposes. *Geosystems and Geoenvironment,* 5 (2026) 100518. https:-//doi.org/10.1016/j.geogeo.2026.100518

Ekanem, A. M., George, N. J., Thomas, J. E. & Udo, I. G. (2024). Geophysical investigation of aquifer flow unit characteristics in northern parts of Akwa Ibom State, Southern Nigeria. Results in Earth Sciences, 2, 100017, ISSN 2211-7148, https://-doi.org/10.1016/j.rines.20-24.100017

Ekanem, A.M., Akpan, A.E., George, N.J. & Jewel E. Thomas (2021a). Appraisal of protectivity and corrosivity of surficial hydrogeological units via geo-sounding measurements. *Environ Monit Assess* **193**, 718 (2021). https://doi.org/10.1007-/s10661-021-09518-9

Ekanem, A.M., George, N.J., Thomas, J.E. & Ekpenyong, N.E. (2021b). Seismic modelling study of CO_2 effects on P-wave amplitude. *Model. Earth Syst. Environ.* **7**, 1693–1701. https://doi.org/-10.1007/s40808-020-00904-9

Ekefre, A. E., George, N. J., Udoh, A. C., Harry, T. A., & Etim, C. E. (2025). Predictive Analysis of Sand Production and Flow Implications using Petrophysical-Geomechanical Properties: A case of "ANY" Field, Niger Delta. *Researchers Journal of Science and Technology*, *5*(2), 54–73. https://doi.org/10.83080/rejost.-vol5no2.174

Evamy, B. D., Haremboure, J., Kamerling, P., Knaap, W.A., Molloy, F.A., & Rowlands, P. H., (1978): Hydrocarbon habitat of Tertiary Niger Delta: American Association of Petroleum Geologists Bulletin, v. 62, p. 277-298.

Gao, G., Zhang, Y., Yang, Z., Duan, B., Liu, W., Zhang, X., Qiu, X., & Liu, M. (2025). An Innovative Approaches to Fault Sealing Evaluation in the Nanpu No. 1 Structural Belt, Nanpu Depression, Bohai Bay Basin. *Processes*, *13*(1), 259. https://doi-.org/10.3390/pr13010259.

George, N. J. Akpan, A.E. & Akpan, F.S. (2017). Assessment of spatial distribution of porosity and aquifer geohydraulic parameters in parts of the Tertiary – Quaternary hydrogeoresource of south-eastern Nigeria, *NRIAG Journal of Astronomy and Geophysics*, 6 (2), 422-433.

George, N.J. & Bassey N.E (2026). Geoelectric and hydro-geochemical assessments of waterlogging and drainage for soil and agronomic groundwater evaluation at Akwa Ibom State University: Field and laboratory data mining approaches. *Geosystems and Geoenvironment*, 5(1), 100464, https://doi.org/10.1016/j.geo-geo.2025.100464

George, N.J. & Thomas, J.E. (2024) Typification of coastal depositional lithofacies with isophysical and isochemical hydro-sand beds via stratigraphic modified Lorenz plots (SMLP): geohydrodynamical implications and valorization of hydrogeological units. *Acta Geophys.* **72**, 1275–1291. https://doi-.org/10.1007-/s11600-023-01160-y

George, N. J. (2021). Integrating hydrogeological and second-order geo-electric indices in ground-water vulnerability mapping: A case study of alluvial environments. *Appl Water Sci* **11**, 123. https://doi.org/10.1007/s13201-021-01-437-x.

George, N.J., Agbasi, O.E., Umoh, A.J, Ekanem, A.M., Udosen, N. I., Thomas, J.E., Aka, M.U. & Ejepu, J.S. (2025). Enhanced contamination risk assessment for aquifer management using the geo-resistivity and DRASTIC model in alluvial settings, *Cleaner Water*, 3, 100060, https://doi.org/-10.1016/j.clwat-.2024.100060

George, N.J., Bassey, N.E., Ekanem, A.M.& Thomas, J. E. (2020). Effects of anisotropic changes on the conductivity of sedimentary aquifers, southeastern Niger Delta, Nigeria. *Acta Geophys*. 68, 1833–1843 (2020). https://doi.org/-10.1007/s11600-020-00502-4

George, N.J., Ekanem, A.M., Thomas, J.E. & Harry, T. A. (2022a). Modelling the effect of geo-matrix conduction on the bulk and pore water resistivity in hydrogeological sedimentary bed-dings. *Model. Earth Syst. Environ.* **8**, 1335–1349 (2022). https://doi.org/-10.1007/s40808-021-01161-0

George, N.J., Obianwu, V.I., Akpabio, G.T., & Obot, I.B. (2010). Comparison of thermal insulation efficiency of some select materials used as ceiling in building design, Scholars Research Library, *Archives of Applied Science Research*, 2 (3): 253-259

George, N. J., & Thomas, J. E. (2023). Groundwater potential and quality assessments of a coastal environment: a case study of the location of Federal University of Technology Ikot Abasi (FUTIA), Akwa Ibom State, Nigeria. *J Coast Conserv.,* **27**, 31. https://doi.org-/10.1007/s11852-023-00956-w.

George, N.J., Umoh, J.A., Ekanem, A.M., Ogbasi, O. E., Jamel, A. & Thomas, J. E. (2022b). Geophysical-laboratory data integration for estimation of groundwater volumetric reserve of a coastal hinterland through optimized interpolation of interconnected geo-pore architecture. *J Coast Conserv.,* 26, 56. https://doi.org/10.1007/s11852-022-00902-2

Horsfall, O.I., Akpan, M.J., George, N.J. (2024) Reservoir characterization of *GABO* field in the niger delta basin using facies and petrophysical analyses, *Results in Earth Horsfall Sciences*, 2 https://doi-.org/10.1016/j.rines.2024.100038

Lin, T., Dong, Z., & Gong, B. (2025). Numerical Study of the Mechanical Properties and Failure Mechanisms of Shale Under Different Loading Conditions. *Applied Sciences*, *15*(8), 4405. https://doi.org/-10.3390/app15084405

Navarro-Perez, D., Fisher, Q., Lorinczi, P., Velásquez Arauna, A., & Valderrama Puerto, J. (2025). A Review on Greensand Reservoirs' Petrophysical Controls. *Minerals*, *15*(12), 1280. https://doi.org/10.3390/min15121280.

Nwanjide, C.S (2013): Geology of Nigeria's Sedimentary Basins. CSS Bookshops Limited, Lagos.

Obianwu, V.I., Udoh, J. T., George, A. M., & George, N. J. (2015) Seismic Early Warning Foundation Conditions Evaluation Survey for Civil Engineering Constructions in Akpabuyo Local Government Area of Cross River State, Nigeria. *British Journal of Applied Science & Technology*, 6 (6), 583

Short, K. C., & Stauble, A. J. (1967). Outline of geology of Niger Delta. AAPG Bulletin, 51(5), 761–779. https://doi.org/10.1306-/5D25C06D-16C1-11D7-8645000102-C1865D

Tuttle, M.L.W., Charpentier, R.R., and Brownfield, M.E., (1999): The Niger Delta petroleum system: Niger Delta province, Cameroon, and Equatorial Guinea, Africa: http://greenwood.cr.us gs. gov/energy/ Won dEnergy/O F99-5 0H/ChapterA.htm#TOP.

Udo, K. I., George, N. J., Akankpo, A. O., Azuoko, G. B., & Aka, M. U. (2020). Determining fracture pressure gradients from well logs. *Int J Adv Geosci*, *81*(1), 5-9.

Udosen, N. I., Ekanem, A. M. & George, N. J. (2024a). Geophysical exploration to assess leachate percolation and aquifer protectivity within hydrogeological units at a major open dump in Eket, Nigeria, *Results in Earth Sciences*, 2, 100022, ISSN 2211-7148, https://doi.org/10.10-16/j.rines.2024.100022.

Udosen, N. I., Ekanem, A. M., & Thomas, J. E. (2024b). Geo-hydraulic characterization of a coastal aquifer system in South-eastern Nigeria with the inverse slope method. *Researchers Journal of Science and Technology*, *4*(1), 1–20. https://doi-.org/10.83080/rejost.vol4no1.82

Udosen, N.I., Ekanem, A.M., George, N.J. (2024c). Modeling of aquifer geo-hydraulic characteristics with geo-electrical methods at a major coastal aquifer system in Uyo, southern Nigeria. *Water Practice and Technology,* 19 (2): 611–628. https://doi.org/10.2166/wpt.2-024.018

Umoh, J.A., George, N.J., Ekanem, A.M. & Emah J.B. (2025). Characterization of hydro-sand beds and their hydraulic flow units by integrating surface measurements and ground truth data in parts of the shorefront of Akwa Ibom State, Southern Nigeria. *Int J Energ Water Res* **9**, 13–29, https://doi.org-/10.1007/s42108-022-00215-y

Umoren, B. E. & George, N.J. (2018). Time lapse (4D) and AVO analysis: A case study of Gullfaks field, Northern North Sea, *NRIAG Journal of Astronomy and Geophysics*, DOI: 10.1016/j.nrjag.20-18.03.004.

Uwa, U.E., Akpabio, G.T. & George, N.J. (2019) Geohydrodynamic Parameters and Their Implications on the Coastal Conservation: A Case Study of Abak Local Government Area (LGA), Akwa Ibom State, Southern Nigeria. *Nat Resour Res* **28**, 349–367.